Paper wcd-2020-18

Attribution of precipitation to cyclones and fronts over Europe in a kilometer-scale regional climate simulation

Stefan Rüdisühli, Michael Sprenger, David Leutwyler, Christoph Schär, and Heini Wernli

Response to the Reviewers' comments:

We thank both reviewers for their constructive and helpful comments that helped to further improve the presentation of our results.

Following are detailed replies to the individual comments.

Reviewer #1

This is a very timely paper on attribution of precipitation to main rain-bearing systems. It is not the first attempt to associated precipitation to various synoptic features, but this time it is more detailed and done using outputs of a convection-resolving model. I also like that results show annual and seasonal data for all 4 seasons, as there are important seasonal differences. The manuscript features excellent literature review and is well written.

Many thanks for these positive statements!

I have relatively minor comments listed below. I am most concerned about attributing precipitation to high pressure systems. As the authors say, it is most likely associated with convection, so I made a few suggestions on that in the comments. Another suggestion is to add a threshold on the size of frontal areas, as there are many very small frontal features in the examples. Finally, I am interested if similar approaches are applied to ERA5 (or other reanalyses), how the results will be different. The latter might be outside the scope of this paper, so I wish to see such comparison sometime in the future.

We address all these points below.

Comments:

1. l.158, 185: The 12 km domain is not significantly larger than 2.2 km domain. Did you consider merging with ERA-interim? It might be particularly good for getting cyclones and high-pressure systems right.

While indeed the difference in domain size between the 2.2 km and the 12 km simulation is not huge, it still makes a large difference for the cyclone identification because the influence of the domain boundary on cyclone feature growth is largest in the direct vicinity of the boundary.

In fact, we have previously investigated the influence of the domain boundary on the cyclone identification (see Rüdisühli (2018), https://doi.org/10.3929/ethz-b-000351234), comparing cyclones identified in ERA-Interim (on a global grid), the 12 km simulation, and the 12 km simulation with a reduced domain size (minus 40 grid points in all directions, corresponding to the domain of the 2.2 km simulation, but without including any 2.2 km data). The absolute cyclone frequencies are shown in the following figure:

ERA-Interim	12 km	12 km – 40 pt
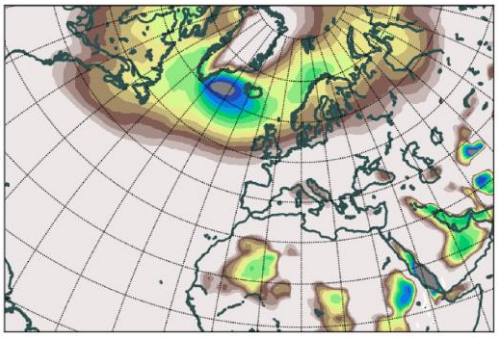	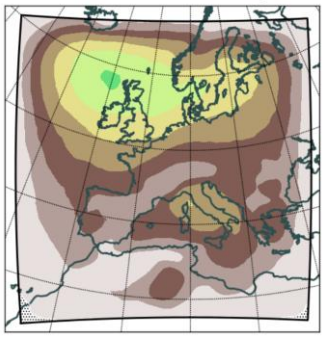	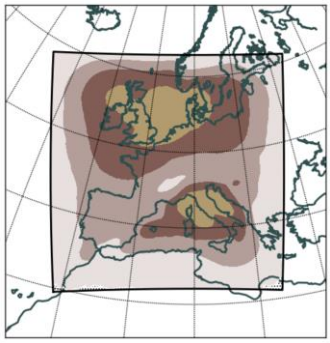
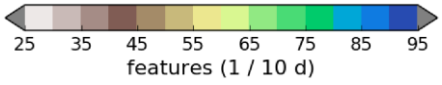	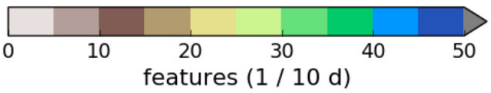	

Note that the absolute frequencies between ERA-Interim and the 12 km simulation are not directly comparable, as we did not account for differences in grid resolution etc. Also note that differences in feature frequency are largely caused by differences in the mean feature size rather than differences in the occurrence frequency of the features. In other words, the 12 km simulation has a similar number of cyclones as ERA-Interim, e.g., near Scotland, however they are smaller (because of the limited domain) and therefore the frequencies are lower.

But most relevant here is the comparison of the two 12 km composites. It is obvious that the reduced domain size has a large impact on the cyclones over the North Atlantic, whereas the frequencies are very similar over the southern half of the domain. The influence of the boundary becomes even more obvious if we look at the ratio of the above cyclone frequency fields from the 12 km simulation:

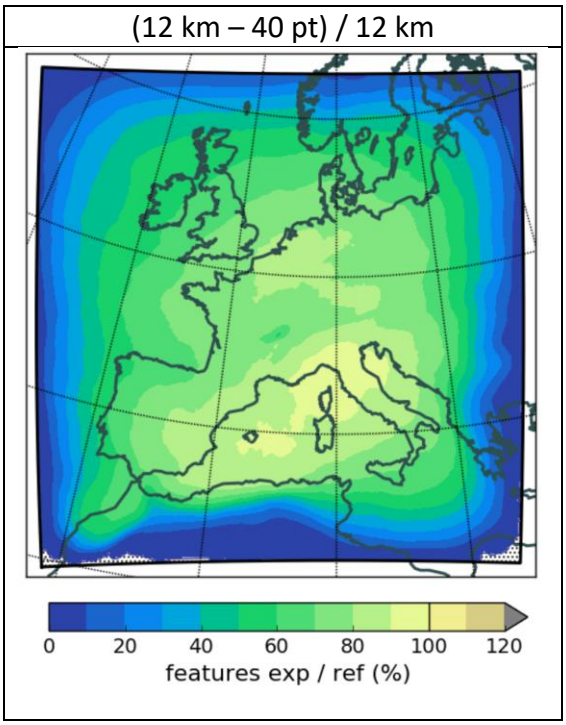

The figure clearly reveals the strong boundary influence, as the cyclones very rapidly decrease in size (and thus composite frequency) very close to the boundaries.

These comparisons give an idea of the benefit of increasing the domain size, in particular for the northern part of the model domain where cyclones typically propagate rapidly across the domain. Properly tuned, increasing the domain size of the 12 km domain using ERA-Interim – as suggested by the reviewer – may have a similar effect as increasing the 12 km domain from reduced to full size, with a large effect in a narrow boundary zone and a smaller effect in the interior of the domain.

In conclusion: Yes, there would likely be a benefit on the identified cyclones by increasing the domain further with ERA-Interim, but already the relatively small increase from the 2.2 km to the 12 km domain has a substantial positive effect on the cyclones in the analysis domain, removing the worst of the boundary effect (as shown above). This is why we decided that the additional effort of incorporating ERA-Interim data was not worth it; while certainly not perfect, for our purposes (of distinguishing the zone close to the cyclone center from the rest of a cyclonic system) the identified cyclones are good enough.

For our high-pressure areas, on the other hand, extending the domain further would not make any difference, as they are based on the local values of the geopotential field and its gradient (see also our answer to comment 5).

2. l.193-194: This not clear. Please explain better what you mean by allowing 20% of contours to cross the boundary before 'halting further feature growth'.

We agree and have changed the text to express this more clearly.

Old:
[...] We opt for a compromise by allowing one in five contours of a feature (20 %) to cross the boundary before halting further feature growth.

New:
[...] We opt for a compromise by allowing up to 20 % of the contours of a feature to be boundary crossing. For example, if 16 closed contours are identified around a pressure minimum before the boundary is reached, then at most four additional boundary-crossing contours can be added before the 20 % threshold is reached at four out of twenty contours.

3. l.200: In the abstract it is said that local thermal fronts are removed, here you say that fronts are categorised at synoptic and local. Are local fronts removed then?

Yes, the local fronts are removed for this analysis. We have added a sentence to emphasize this.

New:
The local fronts are then removed and only the synoptic fronts are used in this study.

4. l.215: What is the threshold value on theta-e gradient based on and why all values in Table 1 are whole numbers?

This is a good question, pointing to the challenge of reasonably choosing the theta-e gradient thresholds. To the best of our knowledge, there is no fully objective procedure to determine these thresholds. We found the monthly threshold values subjectively by examining multiple years of data. Specifically, we have evaluated the fronts based on a range of possible thresholds, deduced monthly "best estimates" based on how well the front features matched the meteorological fields, and based on these determined the thresholds listed in Table 2. Given their subjective and approximate nature, and their magnitude, there was no reason not to settle on whole numbers. We mention this challenge of choosing appropriate thresholds also in the third bullet point of our conclusions.

5. l.252: It is not clear to me how high-pressure systems are defined. One may think that you mean anticyclones (i.e. an area similar to cyclones with high pressure in the middle circled by a closed contour), but 'high pressure' systems in fig. 3 look confusing. In fig 3 (summer) the green area looks like the subtropical ridge (there are big and small white areas within green stippling - what do they represent?), in fig. 5 (winter) I would suspect an anticyclone defined using the MSLP field. These systems need to be better described, both their identification procedure and physical meaning. There is a recent paper by Poujol et al. (2020) on a separation between convective and stratiform precipitation. It might be interesting to check if the precipitation within high pressure systems can be classified as convective using their approach. Discussion around lines 400 and 463 may benefit if you mention possible convective nature of high-pressure precipitation, that is prevalent in summer. Given the frequency of high-pressure 'components' (fig. S4), which cover 50% of your domain 50% of time in summer, these systems need to be explored in more detail.

The identification procedure of the high-pressure areas is described in Sec. 2.4: They are areas with high pressure (Φ at 850 hPa above threshold derived from monthly values in Table 2, which have been found by a similar subjective evaluation as the frontal gradient thresholds in Table 1) and a flat pressure distribution ($\nabla\Phi < 0.02$ m s^{-2}). As opposed to fronts and cyclones, the high-pressure areas are simple masks, without any sophisticated feature identification or tracking. The white areas within the green stippling in Fig. 3 are therefore regions where either the geopotential is locally too low and/or its gradient is locally too strong.

We agree that the motivation, physical meaning, and name of the high-pressure areas are not explained in sufficient detail. We have revised and extended Sec. 2.4 to more clearly convey these points.

Old:
Precipitation not only occurs near cyclones and fronts, but also in areas of weak synoptic forcing typically characterized by relatively high pressure or by a flat pressure distribution, for example with diurnal summer convection over the continent. We explicitly identify such high-pressure areas based on geopotential Φ and its gradient ∇Φ at 850 hPa. Seasonal feature frequency composites are provided in the supplementary material (Fig. S1).
The Φ field is first smoothed with a Gaussian filter. A mask is derived by applying a minimum threshold that varies over the year to account for the seasonal cycle in Φ. Analogous to the seasonally varying frontal threshold, the Φ threshold values are defined in the middle of each month (Table 2) and linearly interpolated to each hour in-between. Then, ∇Φ is computed, and the resulting field is smoothed again. A second mask is derived by applying a constant maximum threshold of 0.02ms−2 to ∇Φ. The high-pressure area corresponds to the overlap area of the Φ and ∇Φ masks. All threshold values have been determined subjectively based on thorough manual testing.

New:
Precipitation not only occurs near cyclones and fronts, but also in areas of weak synoptic forcing typically characterized by relatively high pressure and a flat pressure distribution, for example with diurnal summer convection over the continent. When attributing precipitation only to cyclones and fronts, such precipitation would not be captured and become part of the residual. Our original method without high-pressure areas, however, often misclassified diurnal summer convection as front-related (specifically far-frontal, as defined in Sec. 2.5). To prevent this, we explicitly identify such areas characterized by high pressure and a flat pressure distribution – henceforth simply called high-pressure areas *– based on the geopotential Φ and its gradient ∇Φ at 850 hPa. Seasonal frequency fields of the identified high-pressure areas are provided in the supplementary material (Fig. S1).*
Computing the high-pressure areas at 850 hPa involves the following steps:

1. *Smooth the Φ field using a Gaussian filter with a standard deviation σ=3. Then compute a Φ mask covering areas with high pressure, based on a minimum threshold, which varies over the year to account for the seasonal cycle in Φ. The threshold at a given time step is derived by linear interpolation from the mid-monthly threshold values listed in Table 2.*
2. *Smooth the Φ field again using a Gaussian filter with a standard deviation σ=20, then compute ∇Φ, whereby the gradient at each grid point is computed across multiple unit grid distances using offsets of (i±10, j±10), corresponding to ±120 km in our hybrid 12 km fields. Then compute a ∇Φ mask covering areas with a weak pressure gradient, based on a constant maximum threshold of 0.02 m s^{-2}.*
3. *The high-pressure area corresponds to the overlap area of the Φ and ∇Φ masks.*

All threshold values have been determined subjectively based on extensive manual evaluation of multiple years of data.

We thank the reviewer for pointing us to the paper by Poujol et al. (2020), as their classification approach looks very promising. However, we do not think that it would add much to the characterization of the high-pressure area precipitation, because it is fairly obvious to us (from extensive visual analysis of precipitation fields during method development) that most of this

precipitation is convective. But their separation of precipitation types could be a great extension of our attribution method, which could be addressed future studies. We have added such a remark to the end of the "Conclusions".

New:
Finally, methods that separate precipitation types like convective and stratiform (e.g., Poujol et al., 2020) could be combined with our feature-based attribution, which would enable a more in-depth characterization of the different front-cyclone-relative precipitation components

References:

Poujol, B., Sobolowski, S., Mooney, P., and Berthou, S.: A physically based precipitation separation algorithm for convection-permitting models over complex topography, Q.J.R. Meteorol. Soc., 146, 748–761, https://doi.org/10.1002/qj.3706, 2020.

6. Fig.3: The example is very good, but I have numerous suggestions on plotting:

- **The red outline stands for local fronts, while red filling (in slightly different shade) - for warm fronts. It would be good to use different colours.**
- **A bold black contour also circles the cyclone area, is that right? I think it is not mentioned in the caption.**
- **Blue filling of cold fronts is very similar to precipitation 0.2-1 mm/h, please use different colours.**

We agree that the plotting is not optimal, especially with respect to the color clashes. In hindsight, we tried to achieve too much at the same time: intuitive colors for cold and warm fronts (blue for cold, red for warm) and for synoptic and local fronts (black for "good", red for "bad"), while still sticking with the same precipitation color map as in all other figures – which, unfortunately, also includes red and blue, as the reviewer has pointed out.

We have therefore adapted the figures as follows:

- Precipitation is shown in shades of gray, which prevents color clashes.
- Cold and warm fronts are now distinguished by the color of their outlines (blue and red), while the filling has been removed because it clashed with the precipitation field, one necessarily obscuring the other.
- Local fronts are now all highlighted by the same outline color (orange), because the type of the local fronts is of secondary importance at best.
- (For Uriah, show the time steps in the figure that are actually described in the text.)

Regarding the caption, cyclones were actually mentioned (*"[...] the unfilled bold contours the outlines of cyclone features; [...]"*), but we concede that the sentence was not easy to read. When rewriting the caption, we have tried to make it more easily understandable.

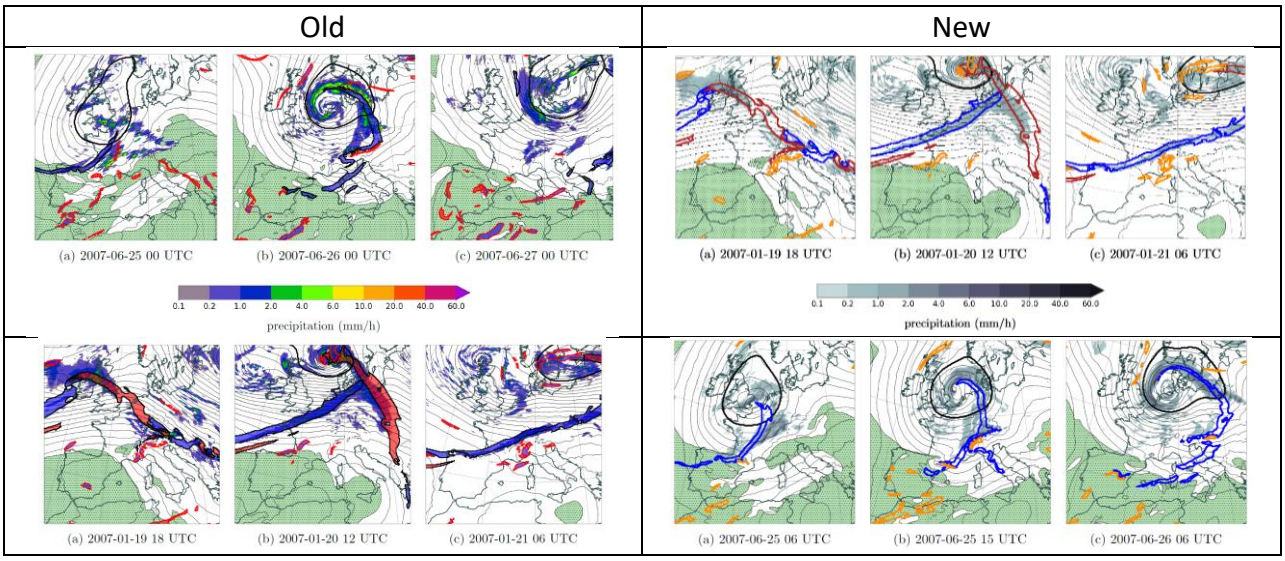

Old:
Figure 3. Development of cyclone Uriah in June 2007. The thin black contours indicate geopotential at 850 hPa; the colored shading the surface precipitation; the filled bold contours the outlines of front features, with black/red outlines for synoptic/local fronts, and blue/red filling for cold/warm fronts; the unfilled bold contours the outlines of cyclone features; and the green stippling high-pressure features.

New:
Figure 3. Development of cyclone Lancelot in January 2007. Thin black contours indicate the geopotential at 850 hPa, gray shading the surface precipitation, and green stippling the high-pressure areas. Bold contours represent the outlines of tracked features: synoptic cold and warm fronts (blue and red), local fronts of either type (orange), and cyclones (black).

- **I am not sure I can see red filling well for the warm front (it works better in fig. 5). Is warm front in fig. 3 a 'local' front, not synoptic? If this is the case then the separation between local and synoptic fronts is probably not working very well.**

Indeed, the warm front in this case is too weak to be robustly classified as a synoptic front. For this particular case, one might thus argue that the classification is not working very well. However, one must keep in mind that the algorithm has not been tuned for this specific case, but such that it does a reasonable job in the majority of cases. We have chosen this June case because it meteorologically contrasts the January case in many respects (slow instead of fast, dominant cold front instead of pronounced warm front, "Norwegian" instead of "Shapiro-Keyser", summer instead of winter), without too much consideration of the performance of the identification algorithm. Our goal is to illustrate the performance of the algorithm in representative – albeit meteorologically attractive – scenarios, rather than "cherry-pick" cases where the algorithm does an especially good job.

That being said, it is indeed not optimal that there is no synoptic warm front in the Figure of the summer case, given they should still be mentioned in the caption. We have therefore decided to switch the two case studies, such that this type of figure can be introduced for the winter case (in which all elements are present) and then referred to by the respective summer case figure.

We have also adapted the text to stress that the warm front is not detected as a synoptic feature by the algorithm and thus not used for the precipitation attribution.

- **It would be good to remind the reader that frontal systems within the high-pressure system do not count as rain-bearing (i.e. this precipitation is attributed to the high-pressure system only).**

We agree and have added a short remark to the caption of Fig. 5: *"Note that in (a), the precipitation along the cold front over northwestern Spain will be attributed to the high-pressure area instead, which takes precedence over fronts (see Sec. 2.5)."*

7. Fig. 3 Makes me think that it would be good to have a threshold on the size of the frontal area to remove very small features.

We definitely tried that. The problem with an explicit feature size threshold is that it harms as much as it helps. While it would surely remove some spurious features that we'd prefer to get rid of, it would also remove many that we do want to retain, for instance fronts associated with small cyclones over the Mediterranean, or fragments of large fronts that are not connected to the main feature. (Fragmentation is fairly common for all but the largest fronts, given most of our domain is over land.)

We tried many different approaches and combinations of criteria, and finally settled on the two criteria described in Sec. 2.3: "typical feature size" and "stationarity". The former does indeed consider feature size, but for whole tracks rather than individual time steps, which makes it more robust in case of fragmentation. The stationarity criterion allows for, e.g., the mobile fronts associated with small Mediterranean cyclones to be classified as non-local and thus make it into the analysis. Fig. 3 actually illustrates that these criteria work fairly well, as most small-scale features are classified as local (red outlines) while the larger, precipitating fronts are classified as synoptic.

8. l.412, Fig 8 vs Fig 9, high pressure precipitation: In figure 8 high-pressure precipitation is over the land only (with an exception for the Bay of Biscay), but for relative precipitation there is a large proportion of convective precipitation over the Mediterranean Sea. Can you explain this?

Yes, we can. Fig. 8 shows absolute precipitation amounts of the components, starting at 0.25 mm/d, while Fig. 9 shows the relative contributions of the components to the absolute precipitation amount. In summer, there is hardly any precipitation at all over the Mediterranean Sea: less than 0.75 mm/d overall, and none of the four shown components exceeds 0.25 mm/d. However, as Fig. 9 shows, there is some precipitation, and a substantial fraction of it is associated with high-pressure areas (i.e., presumably convective). In fall, on the other hand, there is substantially more precipitation over the Mediterranean Sea than in summer with about 1.5 mm/d on average, and the high-pressure contributions locally exceed 0.25 mm/d in several places. The modest about 10% high-pressure contributions in Fig. 9 are thus consistent.

9. Fig. 9: I find it odd that cyclone and far-frontal precipitation are combined in this plot. I am not sure if this information is valuable. Is it possible to separate them?

Yes, it is possible to separate them. We opted to combine them to reduce the number of plots; the focus of the figure is mainly on the other contributions (frontal, high-pressure, residual), so we combined cyclonic and far-frontal into “other front/cyclone-related”.

Upon reflection, we do agree that this is probably not the most meaningful way to combine these groups. We have therefore separated the far-frontal and cyclonic contributions, now showing them separately.

10. l.438: Are you able to explain high amount of residual heavy precipitation comparable to, e.g., cold-frontal heavy rainfall?

The residual is especially large in spring, which is when fronts (especially warm fronts) already occur less frequently than during their peak in winter, but high-pressure areas have not yet reached their peak frequency in summer. Given the larger residual heavy precipitation in spring compared with the other seasons, especially over land, some of this may be due to early convective precipitation events, which are not captured by our high-pressure areas to the degree they are in summer.

Similarly, over Sweden, the large amounts of heavy residual precipitation in spring coincide with a lower cyclone frequency compared with summer. Possibly, convective precipitation events in spring are triggered by other processes than cyclones, while in summer, many are associated with cyclones when those occur with high frequency.

In summer, the residual is distributed fairly evenly across the domain and roughly comparable to the total frontal contributions, while the cyclonic and high-pressure contributions are substantially larger. This is not surprising given the frequency minimum in both cold and warm fronts in summer.

In fall, residual contributions are relatively large over the Baltic states, where the front and cyclone frequencies are much lower than further west. In addition, this is close to the upper-left corner of the domain, so in addition to natural decay of these systems, boundary effects on the feature identification may also play some role.

Finally, from fall through spring residual precipitation is relatively frequent and heavy along the North African coast. Only few cyclones and fronts occur in this region, and the high-pressure area frequency is also much lower than in summer, so most precipitation is classified as residual. However, since this region is drier than most areas further north, large relative residual contributions still translate to relatively little residual precipitation in absolute terms.

Minor comments:

11. Fig. 1 and possibly other plots: Please add lon/lat values.

We agree that the grid lines should be labeled in Fig. 1. We have redone this figure with grid line labels, and in the process also added the inner boundary of the blending zone.

As for the other plots, we are of the opinion that grid line labels do not offer much benefit (the location of the domain is obvious given the European coastlines, the shown grid lines are only major and thus easily deduced from the coastlines, and the domain is the same in all plots), but major downsides (if placed in the plots, it would fill them up even more and make it even harder to deduce details as it already is given their small size, while if placed outside the plots, it would increase the size of the multi-panel figures, potentially necessitating even smaller maps).

Old	New
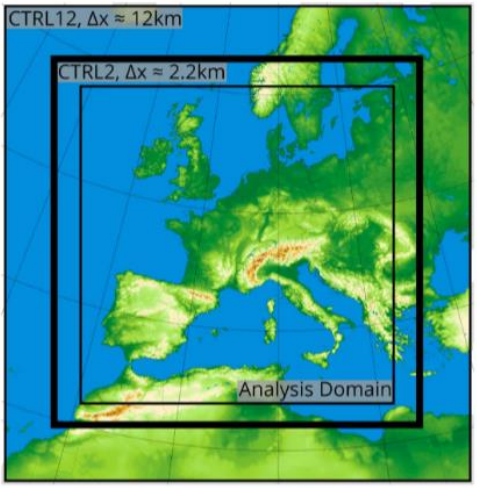	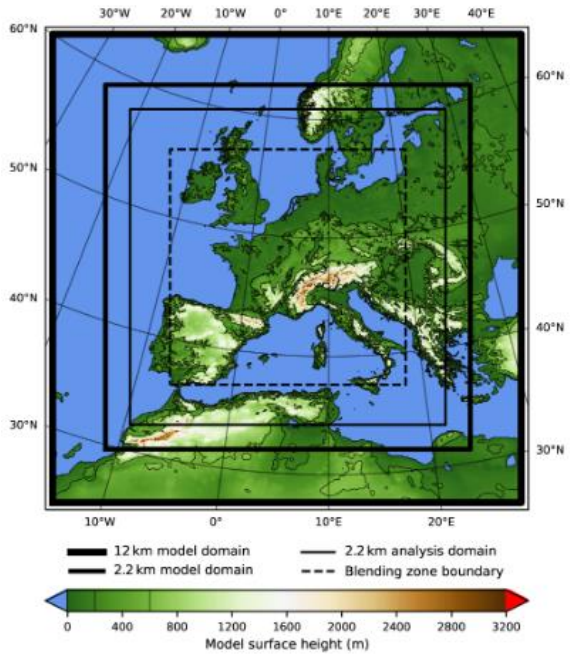

Old:
Figure 1. COSMO simulation domains and model topography. The outermost black box denotes the domain of the convection-parameterizing simulation with a grid spacing of 12 km and the bold box the domain of the convection-resolving simulation with 2.2 km grid spacing. The innermost thin box indicates the subdomain used in the analysis. (Figure and caption from Leutwyler et al., 2017)

New:
Figure 1. Domain boundaries and model topography of the two COSMO simulations. The four black boxes show, from large to small: (bold) the model domain of the driving simulation with a horizontal grid spacing of 12 km; (semi-bold) the model domain of the nested simulation with a horizontal grid spacing of 2.2 km; (thin) the subdomain of the 2.2 km domain on which the precipitation attribution analysis is performed; and (dashed) the inner boundary of the blending zone that is used during the computation of the hybrid fields on which the feature identification is based (see Sec. 2.1). The model topography inside (outside) the 2.2 km domain boundary is that of the nested 2.2 km(driving 12 km) simulation

12. l38: ", high-pressure systems, extratropical cyclones, fronts, orography ... contribute to precipitation" - I'd avoid starting with high pressure systems as they are not the main rain-bearing systems

We agree and have changed it to "[...] extratropical cyclones, fronts, orography, high-pressure systems, and their interactions [...]".

13. l45, l.78, 80: I think it should read "such resolution", "such attribution"

We agree and have changed it as proposed.

14. l47: I'd rather say "interplay between fronts and steep orography in producing precipitation"

We agree and have changed it as proposed.

15. l53-55: I doubt this sentence is needed

We agree and have removed the sentence.

16. l.98: Re-phrase 'on a continental-scale domain'; perhaps, 'for a continental-size domain' or "on a scale of a continent'

We agree this could be phrased better and have changed it to "at a continental scale".

17. l.114: 'domain covering most of Europe' - I disagree, though it is hard to get the area by eye. Given the size of Eastern Europe (former USSR seems to be excluded from analysis) and Scandinavian counties, my feeling is that the domain covers roughly half of Europe.

We agree that the domain does not cover Eastern Europe, but Western Europe and a large fraction of the Mediterranean. We have therefore changed "the comparatively large domain covering most of Europe" to "the decade-long simulation on a computational domain capable of representing the evolution of these systems over Western Europe, the eastern North Atlantic, and the Mediterranean".

We note that the computational domain covers an area of about 11,000,000 km^2, which is a bit larger than the European land area.

18. l.124: "this attribution" replace with "their contribution"

We partially agree and have changed it to "these contributions".

19. l.133: 'can be found' instead of 'is found'

We agree and have changed it as proposed.

20. l.156: Replace interpolate with extrapolate

Given this transformation step is only performed over the part of the 12 km grid covered by the 2.2 km grid, where we have data, we think that "interpolate" is indeed the right word. However, we concede that the whole explanation of the procedure could be clearer (see also next comment) and have thus rephrased it.

21. l.165: "the features are interpolated back onto the original 2.2 km grid". I do not think this is the right way of describing it. My understanding is that you first create a mask based on 12 km field and then use it on 2.2 km scale.

Indeed, the feature masks are first created on the 12 km grid based on the "hybrid fields" and then used at 2.2 km scale to attribute the precipitation fields from the 2.2 km simulation to the features. Technically, this involves interpolating the feature masks from the 12 km to the 2.2 km grid (where the data in the interior of the domain has originally come from, thus the "back"). We have rephrased the explanation of the whole procedure (see also previous comment) to make it clearer and more precise.

Old:
[...] In order to exploit the advantages of both simulations, the 2.2 km and 12 km data are merged in the following three-step procedure:

1. *Interpolate the 2.2 km fields onto the 12 km grid. This retains the exact position and extent of the cyclones and fronts in the 2.2 km simulation while increasing the signal-to-noise ratio to the level of the 12 km simulation.*
2. *Paste these into the 12 km fields to obtain hybrids comprised of 2.2 km simulation data in the center and 12 km simulation data beyond the boundaries of the inner nest.*
3. *Introduce a blending zone along the boundaries in the inner domain with a smooth transition from the 2.2 km data to the 12 km data. It extends 50 coarse grid points (~60 km) into the inner domain and is based on the logistic function1/(1 + exp−k×x) with k= 0.8.*

This retains the exact position and extent of the cyclones and fronts in the 2.2 km simulation while increasing the signal-to-noise ratio to the level of the 12 km simulation. The resulting hybrid fields reside on the grid of the 12 km simulation and thus benefit from its large domain and relatively low noise level, while being meteorologically consistent with the 2.2 km simulation within the analysis domain in the inner nest. We use them to identify cyclones (Sec. 2.2) and fronts (Sec. 2.3). Before conducting the precipitation attribution analysis (Sec. 2.5), however, the features are interpolated back onto the original 2.2 km grid.

New:
[...] In order to exploit the advantages of both simulations, the 2.2 km and 12 km data are merged in the following procedure:

1. *Interpolate the 2.2 km fields to the part of the 12 km grid covered by the domain of the 2.2 km simulation.*
2. *In the interior of the domain at a distance of at least 50 coarse grid points (~600 km) from the boundary of the 2.2 km domain, use these fields from the 2.2 km simulation.*
3. *Outside the 2.2 km domain, use the fields from the 12 km simulation.*
4. *In-between, blend the fields with f= 0.1/(1 + exp (−0.8 × (10x − 5))), where x increases linearly from 0.0 at the inner boundary of the blending zone to 1.0 at the outer boundary and f increases logistically in the same range, corresponding to the fraction of 12 km data*

The resulting hybrid fields possess the bigger domain and lower noise level of the 12 km simulation, which allows for a more robust feature identification over the analysis domain, especially close to the boundaries such as over the North Atlantic. At the same time, the hybrid fields are meteorologically consistent with the 2.2 km simulation.

We use the hybrid fields on the 12 km grid to identify cyclones (Sec. 2.2), fronts (Sec. 2.3), and high-pressure areas (Sec. 2.4), and then use the resulting feature masks at 2.2 km for the precipitation attribution analysis (Sec. 2.5).

22. l.392: Change to 'selected'

We agree and have changed it as proposed.

23. l.558 and throughout the manuscript: I would avoid saying that summer precipitation is 'associated' with high-pressure systems, though technically this is what the paper shows. As you say, it is most likely associated with convection. I'd rather say that summer precipitation is often detected within high pressure systems.

We agree and have adapted this sentence accordingly.

Old:
It is interesting that this approach confirms the strongly opposing character of winter and summer precipitation, the former being very strongly associated with cyclones and fronts, and the latter predominantly with high-pressure systems.

New:
It is interesting that this approach confirms the strongly opposing character of winter and summer precipitation, the former being very strongly associated with cyclones and fronts, the latter predominantly detected within high-pressure systems.

24. Fig. S2: Why do you need 'track frequencies', would simply 'frequencies' not be enough?

No, "frequencies" would be ambiguous. As explained in the respective caption, the "track frequencies" are computed by compositing the track masks (which comprise all grid points that have encountered at least one feature belonging to the track at least once), as opposed to the complementary "feature frequencies" (e.g., Fig. S1), for which all individual feature masks are composited.

25. Fig. S4: Components of what?

"Front-cyclone-relative" components, as in Fig. S3. The domain is separated at each time step into seven masks corresponding to these components (before these masks are applied to the precipitation field). Figs. S3 and S4 show frequency composites of these masks. We have adapted the Figure captions to express this more clarity.

Old:
Figure S3. Frequencies of front-cyclone-relative components during (0) the whole year, (1) winter (DJF), (2) spring (MAM), (3) summer (JJA), and (4) fall (SON) 2000–2008. Shown are the (a) cold-frontal, (b) warm-frontal, (c) collocated, and (d) far-frontal components.
Figure S4. Like Fig. S3, but showing the frequencies of the (e) cyclonic, (f) high-pressure, and (g) residual components.

New:
Figure S3. Frequencies of front-cyclone-relative component masks during (0) the whole year, (1) winter (DJF), (2) spring (MAM), (3) summer (JJA), and (4) fall (SON) 2000–2008. The masks are obtained at each time step by

separating the domain into seven components as described in Sec. 2.5. Shown are the (a) cold-frontal, (b) warm-frontal, (c) collocated, and (d) far-frontal components.
Figure S4. Frequencies of front-cyclone-relative component masks as in Fig. S3, but showing the (e) cyclonic, (f) high-pressure, and (g) residual components.

References:

Poujol, B, Sobolowski, S, Mooney, P, Berthou, S. A physically based precipitation separation algorithm for convection-permitting models over complex topography. Q J R Meteorol Soc. 2020; 146: 748–761. https://doi.org/10.1002/qj.3706

Reviewer #2

General comments

The aim of this study is to use high-resolution data to quantify the precipitation associated with different weather systems over Europe. In general, the authors have achieved this aim. The paper is clear, and the analysis well presented. However, the abstract does not reflect the quantitative aspect of the paper and simply lists the qualitative results, many of which are supported by previously published work in the literature. What is novel about this study is the development of a methodology which can be used to quantify the extent to which, for example, cold fronts produce more heavy precipitation than warm fronts. This kind of quantitative result should be included in the abstract. Furthermore, there is not enough motivation/context for the work, or inclusion of the wider implications. How might the methodology and results impact forecasting, model development, understanding of precipitation? *How might the methodology be used in the future to investigate precipitation in a changing climate?* Finally, while the conclusions contain a nice summary of the methodology and its limitations, no such caveats are applied to the discussion of the climatological results. This study is based on only 9 years of data and there are many studies that have shown that decadal variability in cyclone frequency and location exists. Therefore, these caveats must be included in the discussion since conclusions based on 9-years of data may not represent a longer climatology.

We thank the reviewer for the in-depth assessment of our manuscript and for raising many valid points of criticism. Most of them are addressed in the specific comments below.

As for using the methodology to investigate precipitation in a changing climate, we've discussed this aspect in the last paragraph of the initial submission: "It is, however, an open question whether the attribution to the components will be the same in the future climate. First steps to apply our approach to future climate simulations have been taken; first results have been published (Hentgen et al. 2019) and further publications are underway."

References:

Hentgen, L., N. Ban, N. Kröner, D. Leutwyler, and Schär, C., 2019: Clouds in convection-resolving climate simulations over Europe. J. Geophys. Res. – Atmos., 124, 3849–3870. https://doi.org/10.1029/2018JD030150

Specific comments

1. Lines 70-75. Regarding the interaction with orography, it seems amiss that reference to the seeder-feeder mechanism for generating localised heavy precipitation is missing (e.g. Browning et al. (1973).

We agree and have added a sentence referencing the seeder-feeder process.

New:
In the warm sector ahead of the cold front, precipitation from low-level orographic clouds can be strongly enhanced via the seeder-feeder process (Bergeron, 1965) by precipitation from aloft (Browning et al., 1974, 1975).

References:

Bergeron, T.: On the low-level redistribution of atmospheric water caused by orography, Suppl. Proc. Int. Conf. Cloud Phys., Tokyo, pp 96–100, 1965.

Browning, K. A., Hill, F. F., and Pardoe, C. W.: Structure and mechanism of precipitation and the effect of orography in a wintertime warm sector, Q. J. R. Meteorol. Soc., 100, 309–330, https://doi.org/10.1002/qj.49710042505, 1974.

Browning, K. A., Pardoe, C. W., and Hill, F. F.: The nature of orographic rain at wintertime cold fronts, Q. J. R. Meteorol. Soc., 101, 333–352, https://doi.org/10.1002/qj.49710142815, 1975.

2. Line 117. The authors state that the model is free to evolve precipitation systems that may differ from reality despite being forced at the boundaries by re-analysis data. Have they performed analysis of individual precipitation events? Are convective rather than synoptic scale events more likely to be different from reality? Does this affect the conclusions?

The reviewer is raising a valid concern. As the simulation is driven by imperfect reanalysis data, and uses an imperfect limited-area model, individual precipitation events may significantly deviate from reality. Earlier studies on the topic suggest that for computational domains similar to ours, the quality of RCM simulations is comparable on average to that of an operational 2–3 d operational NWP forecast in terms of the 500 hPa RMS error, both during summer and winter (Lüthi et al., 1996). In terms of daily precipitation, the result will be similar, although the details of high-resolution convective events will be much more strongly affected by the chaotic nature of the underlying dynamics (Hohenegger and Schär, 2007). Nevertheless, as the associated level of error is comparable to or somewhat larger than that of a good reanalysis, we believe that overall the climatological characteristics (i.e., based on decadal statistics) are well captured by the presented simulations.

A detailed case study on the representation of the Kyrill storm in the 12 km and the 2.2 km simulations using the same modeling system is provided in Leutwyler et al. (2016). Analysis of the same storm using the same model has been presented by Ludwig et al. (2015), albeit on a smaller domain. Both studies demonstrate a striking difference in the representation of frontal precipitation between convection-resolving and convection-parametrizing simulations. Both of these studies conclude that the representation at convection-resolving resolution is more physically consistent.

We have added the following sentences to the manuscript (original l.115) to reflect this discussion: “The representation of frontal precipitation in the Kyrill storm was assessed in previous studies (Ludwig et al., 2015; Leutwyler et al., 2016). They concluded that performing simulations at convection-resolving resolution yields a more physically consistent representation of frontal precipitation.”

Assessing the representation of deep convection at convection-resolving resolution is a long and ongoing effort (see Hohenegger et al., 2009; Ban et al., 2014; Prein et al., 2015). For the

presented simulation, a validation is provided in Leutwyler et al (2017), as indicated on l.133 of the original submission.

Regarding the occurrence and development of the fronts and cyclones themselves, we have not conducted any evaluation against observations, nor systematically investigated differences between the 12 km and the 2.2 km simulations. Based on our experience, however, we conclude that large-scale systems like North Atlantic cyclones are largely driven by the boundary conditions and thus represented well compared with reality. The farther from the boundaries and the smaller the systems are, however, the freer they were to evolve independently of the boundary conditions.

We have encountered such an example by chance. A small cyclone developed in the northern Mediterranean, then quickly moved around Italy and hit the Greek coast. Both the 12 km and the 2.2 km simulation simulated this cyclone; however, it developed one day apart in the two simulations almost by the hour. The conditions set by the boundaries were apparently favorable for the genesis and development of this cyclone, but the model had considerable freedom as to the day on which this would happen. (We have not investigated which of the two simulations was closer to reality.) This illustrates that (i) the model has considerable freedom in the interior of the domain to evolve differently than the driving simulation, but (ii) that the boundary conditions still sufficiently constrain the simulation to evolve in a consistent way.

References:

Ludwig, P., J. G. Pinto, S. A. Hoepp, A. H. Fink, and S. L. Gray, 2015: Secondary Cyclogenesis along an Occluded Front Leading to Damaging Wind Gusts: Windstorm Kyrill, January 2007. Mon. Wea. Rev., 143, 1417–1437, https://doi.org/10.1175/MWR-D-14-00304.1.

Ban, N., Schmidli, J., and Schär, C. (2014), Evaluation of the convection-resolving regional climate modeling approach in decade-long simulations, J. Geophys. Res. Atmos., 119, 7889– 7907, doi:10.1002/2014JD021478.

Prein, A. F., Langhans, W., Fosser, G., Ferrone, A., Ban, N., Goergen, K., Keller, M., Tölle, M., Gutjahr, O., Feser, F., et al. (2015), A review on regional convection-permitting climate modeling: Demonstrations, prospects, and challenges, Rev. Geophys., 53, 323– 361. doi:10.1002/2014RG000475.

Hohenegger, C., P. Brockhaus, C. S. Bretherton, and C. Schär, 2009: The Soil Moisture–Precipitation Feedback in Simulations with Explicit and Parameterized Convection. J. Climate, 22, 5003–5020, https://doi.org/10.1175/2009JCLI2604.1.

Lüthi, D., Cress, A., H.C. Davies, C. Frei and C. Schär, 1996: Interannual Variability and Regional Climate Simulations. Theor. Appl. Climatol., 53, 185-209

Hohenegger, C. and C. Schär, 2007: Atmospheric predictability at synoptic versus cloud-resolving scales. Bulletin American Meteorol. Soc., 88 (11), 1783-1793, http://dx.doi.org/10.1175/BAMS-88-11-1783

3. Line 143. How frequently are the boundaries forced by ERA-Interim data?

They are updated every 6 h (as available from the ERA data set). Thank you for pointing out that this information is missing. We have added it to the text.

Old:
The coarser COSMO simulation in turn is driven at the boundaries by global ECMWF Interim Reanalysis data available on a 1° grid (Dee et al., 2011).

New:
The coarser COSMO simulation in turn is driven at the boundaries by global ECMWF Interim Reanalysis data available on a 1° grid every 6 h (Dee et al., 2011).

4. Line 145. Is the model orography at different resolution for the 12km and 2.2km resolution simulations? If so, does this affect the results?

The orography differs between the driving ERA-Interim data, the 12 km simulation, and the 2.2 km simulation. While in response we expect significant local differences in precipitation, for instance in the vicinity of the Alps (see Heim et al. 2020 for a more thorough discussion), the larger-scale differences are expected to be small and locally confined, as the simulation is still sufficiently constrained by the lateral boundary conditions.

We have added these remarks to the text.

Regarding the analysis presented in the paper, please note that fields from the 12 km simulation (which are influenced by its orography) are only directly used during front and cyclone identification near and beyond the boundary of the 2.2 km simulation (hybrid fields described in Sec. 2.1; see also comment #21 by reviewer #1). The differences in orography may thus have some influence on the identified fronts and cyclones in places that expose high orography and are located close to the domain boundary. However, given that the 2.2 km fields are first interpolated onto the 12 km grid and in many cases additionally smoothed before the identification step, we do not expect a substantial impact on the identified features. The precipitation analysis in turn only uses data from the 2.2 km simulation and is thus not affected by the difference in orography.

References:

Heim, C., D. Panosetti, L. Schlemmer, D. Leuenberger, and C. Schär, 2020: The Influence of the Resolution of Orography on the Simulation of Orographic Moist Convection. Mon. Wea. Rev., 148, 2391–2410, https://doi.org/10.1175/MWR-D-19-0247.1.

5. Line 158. What do the authors mean by 'Paste' these into the 12km fields?

We have rephrased the explanation of the whole procedure for more clarity in response to comment #21 by reviewer #1.

6. Line 176 and 241. What is the width of the Gaussian filter? Was this an arbitrary choice or was some sensitivity testing performed to gain an optimal choice?

We have used the function "gaussian_filter" from the Python package "scipy.ndimage" (see https://docs.scipy.org/doc/scipy/reference/generated/scipy.ndimage.gaussian_filter.html) with standard deviations parameter "sigma" of:

- 7 for the geopotential field used to identify cyclones (l.176),
- 3 for the geopotential field used for the pressure component of the high-pressure areas (l.241), and
- 20 (on top of the 3) for the same geopotential field before computing its gradient for the pressure gradient component of the high-pressure areas (also l.241).

Note that we have revised the section on high-pressure areas extensively in response to comment #5 of reviewer #1, including a more detailed description of when which fields are smoothed to what degree.

The smoothing parameters were found by extensive manual testing, i.e., they were neither arbitrary, nor optimized by some objective measure, but an optimal choice based on subjective judgement.

7. Line 208. Which input fields are the authors referring to? Could they be more specific please?

This is indeed formulated misleadingly, thank you for pointing this out. We have adapted the text to clearly portray that only the thermal input field (theta-e) is smoothed.

Old:
Input fields are smoothed with the diffusive filter described by Jenkner et al. (2010) with 160 repetitions. Further noise reduction is achieved by computing the gradient at each grid point across multiple unit grid distances using offsets of (i±4,j±4)instead of (i±1,j±1).
The frontal areas are derived from a thermal and a wind component:

- *The thermal component is based on $|\nabla\theta|$ at 850 hPa, from which a mask is derived by applying a minimum threshold. The latter varies over the year to account for the strong seasonal cycle of humidity (and therefore of θ_e) leading to substantially lower cross-frontal θ_e gradients in winter than in summer, and thus far fewer winter than summer fronts for a given threshold (Rüdisühli, 2018). A threshold value is defined in the middle of each month (Table 1) and linearly interpolated to each hour in-between.*
- *[...]*

New:
The frontal areas are derived from a thermal and a wind component:

- *The thermal component is based on θ_e at 850 hPa. The θ_e field is first smoothed with the diffusive filter described by Jenkner et al. (2010) with 25 repetitions. Then a mask is derived from its absolute gradient $|\nabla\theta_e|$ by applying a minimum threshold, which varies over the year to account for the strong seasonal cycle of humidity (and therefore of θ_e) that leads to substantially lower cross-frontal θ_e gradients in winter than in summer and thus far fewer winter than summer fronts for a given threshold (Rüdisühli, 2018). A $|\nabla\theta_e|$ threshold value is defined in the middle of each month (Table 1) and linearly interpolated to each hour in-between.*
- *[...]*

8. Line 225. Why are short-lived fronts discarded in this study? Do they contribute to local precipitation, for example precipitation can sometimes be seen at the leading edge of sea-breeze fronts which are short lived?

Some short-lived fronts looked rather spurious (they just fulfilled the front detection threshold at one time step) and we decided to remove them. This comes at the cost that also some physical short-lived fronts, e.g., related to the see-breeze circulation have been eliminated from our analysis.

9. Line 231. I didn't follow the reasoning for defining local fronts by their size and stationarity. Surely it would be more logical to present the definition of synoptic fronts as large and non-stationary and thus assume the remainder are local (if they occur close to orography or coastlines) rather than the other way around.

The reason why the criteria focus on the local fronts is that the primary motivation to introduce this distinction in the first place was to remove the local fronts from the data set as they were so abundant, especially before we switched from using the 2.2 km data to the hybrid fields on the 12 km grid. However, we agree that it would indeed be more intuitive to focus the grouping on the synoptic rather than the local fronts, and have adapted the text accordingly. (We have also inverted the definition of *stationarity* such that it increases, rather than decreases, with higher values.)

Old:
[...] Local fronts – largely produced by differential heating along topography and coasts – are generally smaller and more stationary than synoptic fronts. These properties can be expressed by a pair of criteria (on which we have settled after extensive manual testing):

- *The* typical feature size *of a track is calculated by first combining, at each time step, the sizes of all features that belong to the track; and then calculating the median of these total sizes over all time steps. Front tracks are considered local if the* typical feature size *does not exceed 1000 km^2.*
- *The* stationarity *of a track is determined as its total footprint area (defined by all grid points that belong to the tracked front at any time) divided by the* typical feature size*. Front tracks are considered local if the* stationarity *does not exceed 6.0.*

All tracks fulfilling one or both criteria are considered local fronts, and thus small and/or stationary. All remaining tracks are considered synoptic fronts, and thus both large and non-stationary.

New:
[...] Synoptic fronts are generally larger and more mobile (i.e., less stationary) than local fronts, which are largely produced by differential heating along topography and coasts. These properties can be expressed by a pair of criteria (on which we have settled after extensive manual testing):

- *The* typical feature size *of a track is calculated by first combining, at each time step, the sizes of all features that belong to the track; and then calculating the median of these total sizes over all time steps. Front tracks are only considered synoptic if the typical feature size is at least 1000 km^2.*
- *The* stationarity *of a track is determined as the typical feature size divided by the total footprint area (defined by all grid points that belong to the tracked front at any time). Front tracks are only considered synoptic if the stationarity is below 0.167.*

All tracks fulfilling both criteria are considered synoptic fronts, and thus both large and mobile. All remaining tracks are considered local fronts, and thus small and/or stationary. Only synoptic fronts are used for the precipitation attribution analysis, while local fronts are removed.

10. Line 267. For the far-frontal precipitation, do these features need to be also within a cyclone mask, or are both local and synoptic fronts included in this classification?

Local fronts are not included in the analysis, only those fronts classified as synoptic. We have added a sentence stating this explicitly at the end of Sec. 2.3 (see answer to comment #9).

The front-cyclone-relative components are defined in the order listed in Sec. 2.5. The far-frontal component is defined second-to-last before only the residual, and thus does not include any grid points that have already been assigned to any other component, including the cyclonic.

(We're assuming that by "features", the reviewer is referring to "precipitation features", rather than front or cyclone features.)

11. Line 273. During the subjective evaluation of the distance thresholds, was any seasonality identified? I.e. did similar thresholds capture the frontal precipitation in both winter and summer?

We did not specifically evaluate the seasonality of the distance of the precipitation to the fronts. However, if there were a pronounced seasonality that substantially exceeded case-to-case variability, we would probably have noticed it. But it must be stressed that such constant distance thresholds don't easily capture all precipitation even within a given system -- let alone for different systems -- regardless of the season, which is part of the reason we opted for a two-threshold approach in order to focus on the precipitation close to the fronts while still capturing that at a greater distance as "far-frontal".

12. Figure 2. This schematic implies that cyclonic and cold frontal precipitation are mutually exclusive. I guess this is not necessarily true, especially during the early stages of cyclone evolution. Also, given the cyclone is part of a larger-scale wave pattern, the location and shape of the high-pressure region in the schematic seems a little odd. What is the reasoning behind the shape and position of the high-pressure region in the schematic?

Cyclonic and cold-frontal precipitation are, by our definition, indeed mutually exclusive. Of course, there is also precipitation which is simultaneously cold-frontal and cyclonic, and in principle we could further subdivide the cyclonic contributions into "purely cyclonic", "cyclonic/cold-frontal", etc. However, this would only further increase the number of components, which is already high enough at seven.

As for the schematic, it aims to represent some characteristics of high-pressure areas (as we defined them) as observed in our data and represented in the case studies (see figure below). In addition, the schematic shows the high-pressure region to overlap the far-frontal area, which highlight its precedence over the latter.

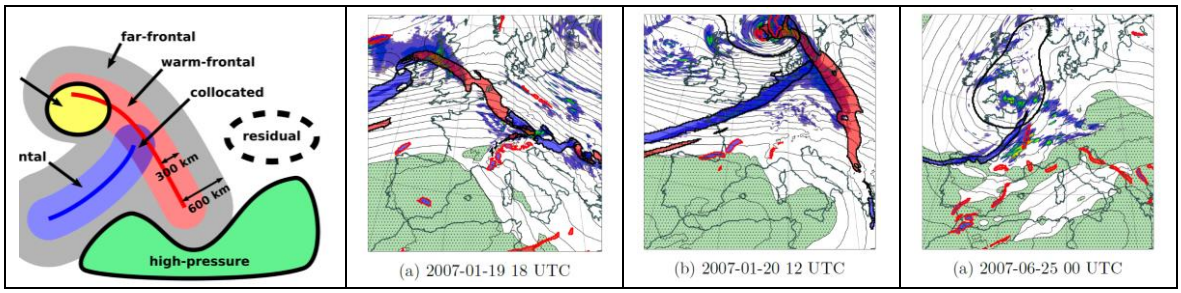

That being said, we do agree that the shape of the high-pressure area in our schematic turned out somewhat peculiar, and we have therefore redrawn the schematic high-pressure area. In addition, we have extended the caption to highlight that the components are, indeed, mutually exclusive.

Old	New
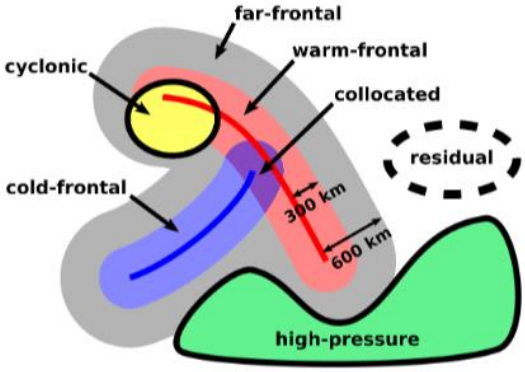	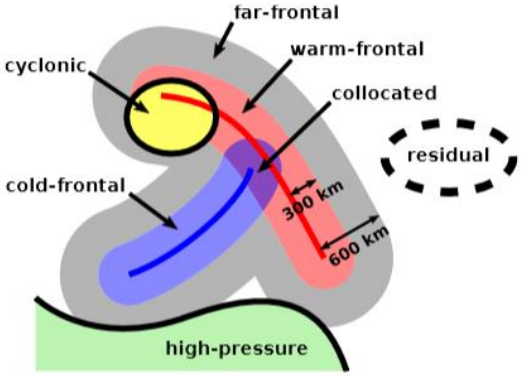

Old:
Figure 2.Schematic depiction of the seven front-cyclone-relative components high-pressure, cyclonic, cold-frontal, warm-frontal, collocated, far-frontal, and residual, as defined in Sec. 2.5.

New:
Figure 2.Schematic depiction of the seven front-cyclone-relative components high-pressure, cyclonic, cold-frontal, warm-frontal, collocated, far-frontal, and residual, as defined in Sec. 2.5. Note that they are mutually exclusive and cover the whole domain, i.e., at a given time step, each grid point is assigned to exactly one component.

13. Figure 3. This figure is too small to see the detailed frontal precipitation features.

Since the reader can zoom in into the high-quality PDF, it should be possible for them to see the important features.

14. Line 289. I do not see the warm front identified in figure 3b. If I understand correctly, this would be a red filled black contour. Where is this feature on the figure?

The warm front is at this time step indeed not identified as a synoptic warm front, only as a local one (red contour). That's why we refer to it in the text merely as "a feature", which may be local or synoptic. "Warm front" in this sentence refers to what we know is there, not to what

the algorithm identifies (or doesn't). We concede that this sentence is not clear enough and have adapted it.

Old:
The warm front east of the cyclone, now detected as a feature, is much weaker than the cold front and produces no precipitation, except close to the cold front, where occlusion may have commenced.

New:
The weak warm front east of the cyclone – now detected, albeit only as a local front – is much less pronounced than the cold front and produces no precipitation, except close to the cold front, where occlusion may have commenced.

15. Lines 295-300. In figures 3b and 3c there is a lot of precipitation that would generally be associated with the occluded/bent-back warm front which is not associated with frontal features using the objective criteria, nor within the cyclone feature contour. Which classification does this precipitation fall into? From figure 4 it looks to fall into the residual. This does not seem correct to me but is not referred to by the authors.

In Fig. 3b, the whole bent-back portion of the precipitation band – actually most precipitation – is inside the cyclone contour and therefore classified as cyclonic. Note that we do mention that this missing front does not seem correct (l.295ff, "The precipitation band along its bent-back portion wraps almost completely around the cyclone center, much farther than the respective front feature, which suggests that not the whole front has been detected as a feature by our algorithm."), although in this case it would not make a difference as the cyclonic component takes precedence over the frontal ones in our algorithm.

In Fig. 3c, on the other hand, the remnants of the precipitation behind the cyclone center fall just outside the cyclone contour. However, there is a small cold-frontal feature east of Scotland, so at least some of this precipitation will be cold- and far-frontal. The southern part of this precipitation area presumably contributes to the residual precipitation feature in that area shown in Fig. 4h.

It is true that we do not explicitly refer to the residual precipitation in Fig. 3c. However, precipitation that should subjectively have been attributed to a cyclone or front but wasn't because the algorithm is not perfect is an inherent part of the residual component. Given the miss in Fig. 3c is, in our opinion, not egregious, we did not specifically comment on it. It would have been a completely different story, of course, if indeed the whole precipitation area bent around the cyclone center in Fig. 3b had been misclassified as residual; that definitely would require a comment.

16. Figure 5. Similar to the comment above, in figure 5a there is a lot of precipitation close to the developing cyclone centre along a bent-back warm front. However, because this cyclone does not have a closed contour it is not captured by the cyclonic criteria. Would this just be assigned to the residual?

In Fig. 5a, only the precipitation beyond 600 km from the outline of the warm front would be classified as residual, which likely captures most of this precipitation, so it will be classified as a

mixture of collocated, warm-frontal, and far-frontal. While there is indeed some residual precipitation in this area, as shown in Fig. 6h, that precipitation mostly stems from post-frontal precipitation and the secondary system visible around the British Isles in Fig. 5b and c.

17. Line 327. What do the authors mean by the 'dry gap region between the fronts'? Is this the warm sector of the cyclone?

No, this refers to the region between the tip of the cold front and the warm front that is oriented perpendicularly to it. However, it is indeed not well visible at the selected time steps – it would be more clearly visible in-between Figs. 5a and 5b. We have removed this sentence because it is indeed more confounding than helpful.

18. Line 330. Browning and Roberts (1997) has a nice description of these cold frontal line features.

Thank you for pointing this out, it is very interesting indeed. We have added a brief reference to that paper.

Old:
In the cold sector behind the cyclone, there is widespread patchy precipitation, some of it associated with a relatively shallow cyclone near the British Isles.

New:
In the cold sector behind the cyclone, there is widespread patchy precipitation, some of it associated with a relatively shallow cyclone near the British Isles in a way reminiscent of secondary cold-frontal lines as described for instance by Browning et al. (1997).

Reference:

Browning, K. A., Roberts, N. M., and Illingworth, A. J.: Mesoscale analysis of the activation of a cold front during cyclogenesis, Q. J. R. Meteorol. Soc., 123, 2349–2374, https://doi.org/10.1002/qj.49712354410, 1997.

19. Line 340. It would be interesting to speculate if any of the precipitation occurring along the northern flank of the Alps was enhanced by precipitation from the frontal clouds falling through orographically generated clouds.

We agree that this would be interesting, but such an analysis is beyond the scope of this study. It would also require cloud and precipitation data at multiple levels, which have not been archived for this simulation and would therefore have to be re-simulated.

20. Line 362. There are also large precipitation amounts over fairly modest topography in the domain. For example, in the UK.

We agree that some of the topography experiencing large amounts of precipitation is short of "high" but merely "modest", and have rephrased it accordingly.

Old:

The largest amounts, however, occur over high topography, especially the Alps, the Dinaric Alps, the Norwegian Alps, the Scottish Highlands, and the Pyrenees.

New:
The largest amounts, however, occur over modest to high topography, especially the Alps, the Dinaric Alps, the Norwegian Alps, the Scottish Highlands, and the Pyrenees.

21. Figure 9 and lines 410-415. In this section the relative contribution from different features to the total precipitation climatology is discussed. This quantitative analysis is surely one of the most novel parts of this work and should be reflected in the abstract.

We fully agree and thank you for pointing this out. We have adapted the abstract accordingly.

Old:
[...] The climatological analysis for the nine-year period shows that frontal precipitation peaks in fall and winter over the eastern North Atlantic, with cold frontal precipitation also being crucial year-round near the Alps; cyclonic precipitation is largest over the North Atlantic (especially in summer) and in the northern Mediterranean (except in summer); high-pressure precipitation occurs almost exclusively over land and primarily in summer; and the residual contributions uniformly amount to about 20 % in all seasons. Considering heavy precipitation events (defined based on the local 99.9th percentile) reveals that high-pressure precipitation dominates in summer over the continent; cold fronts produce much more heavy precipitation than warm fronts; and cyclones contribute substantially, especially in the Mediterranean in fall through spring and in Northern Europe in summer.

New:
[...] The climatological analysis for the nine-year period shows that frontal precipitation peaks in winter and fall over the eastern North Atlantic and the Alps (>70 % in winter), where cold frontal precipitation also being crucial year-round; cyclonic precipitation is largest over the North Atlantic (especially in summer with>40 %) and in the northern Mediterranean (widespread>40 %); high-pressure precipitation occurs almost exclusively over land and primarily in summer (widespread 30-60 %, locally>80 %); and the residual contributions uniformly amount to about 20 % in all seasons. Considering heavy precipitation events (defined based on the local 99.9th percentile) reveals that high-pressure precipitation dominates in summer over the continent (50–70 %, locally >80 %); cold fronts produce much more heavy precipitation than warm fronts; and cyclones contribute substantially (50–70 %), especially in the Mediterranean in fall through spring and in Northern Europe in summer.

22. Lines 420-425. The difference between the regions dominating heavy precipitation and overall precipitation is very interesting.

Thank you, we agree!

23. Line 436. Do the authors have a hypothesis for why cyclonic precipitation is not enhanced by topography in contrast to cold frontal precipitation?

No, unfortunately we don't have a convincing explanation for this.

24. Figure 7d. Does the lack of heavy precipitation associated with collocated fronts mean that ascent of warm conveyor belt over the warm front does not lead to heavy precipitation? This is surprising to me.

We also expect that the ascent of WCBs over the warm front can lead to heavy precipitation, and Fig. 6d provides a nice example for this. Our assumption is that climatologically this ascent

over the warm front occurs more often over the identified warm fronts than the relatively small frontal segments classified as “collocated”.

25. Lines 495-508. This section is a repetition of your results and not a conclusion. I suggest removing this text.

We agree that this section is not strictly necessary and have removed it.

Old:
[...]
The meteorological results of the precipitation attribution show that different components are important in different geographical regions and in different seasons. When considering precipitation over the entire year, the most relevant weather systems are cold fronts near the Alps, warm fronts and cyclone centers in the North Atlantic and Western Europe, and cyclones in the Mediterranean, in particular near Italy and the Balkans. A substantial residual exists (about 20–30 %), indicating that our weather system categories do not encompass all precipitation-producing flow situations and that the attribution to the target systems is not perfect. Strong local enhancement occurs over high topography compared to the surrounding flat areas, 500 which is especially pronounced over the Alps and for cold-frontal precipitation. From a seasonal perspective, (i) cold fronts are important contributors in all seasons (especially over the continent), while warm fronts primarily contribute in winter and fall (especially over the North Atlantic); (ii) the largest cyclonic contributions shift from the Mediterranean in winter to Northern Europe in summer; and (iii) high-pressure precipitation is confined to summer over the continent, with pronounced local enhancement over the Alps. Focusing only on heavy-precipitation events reveals substantial differences to total precipitation: (i) Rather than over high-topography, heavy precipitation is particularly enhanced over land compared to sea; (ii) cold fronts also contribute substantially to heavy precipitation, whereas the relevance of warm fronts diminishes; (iii) cyclones are particularly important for heavy precipitation over the ocean; and (iv) the summertime high-pressure systems further gain in significance, in particular for continental summer convection. The results can be summarized concisely for several distinct geographical regions. [...]

New:
[...]
The meteorological results of the precipitation attribution can be summarized concisely for several distinct geographical regions. [...]

26. Lines 510-550. This section is interesting but should be strongly caveated by the fact that only 9-years of data has been used to create the climatologies. For example, there are many studies demonstrating decadal variability in the latitude of the storm track which would have a large influence on these conclusions.

As regards summer precipitation events, previous studies suggest that the climatology is reasonably well captured by 10-year-long simulations (e.g. Ban et al. 2015, supplemental information), but for the winter seasons significant decadal variations of the NAO indicate that longer periods are indeed desirable or needed to compile a “real climatology”.

To make this point, we have added the following sentences after the regional summary (line 559):

New:
When summarizing these characteristics, it is important to mention another caveat: the comparatively short analysis period of nine years. While interannual variations in summer precipitation appear reasonably well covered with such simulations, variations in the North Atlantic oscillation suggest that longer integration

periods are desirable or needed in order to adequately cover decadal variations of the winter season. A significant challenge of such analyses is the costs of storing high-resolution output of multi-decadal simulations. It is thus desirable to use an online analysis approach that performs the respective analysis while the simulation is running (Di Girolamo et al., 2019; Schär et al., 2020) instead of storing all the relevant output data. Such an online analysis tool can also be highly beneficial when extending the feature-based analyses in three dimensions, e.g., by defining fronts in 3D and/or by considering the vertical structure of clouds and microphysical processes.

References:

Di Girolamo, S., Schmid, P., Schulthess, T., and Hoefler, T.: SimFS: A Simulation Data Virtualizing File System Interface, in: Proc. of the33rd IEEE Int. Par. & Distr. Processing Symp. (IPDPS'19), IEEE, http://arxiv.org/abs/1902.03154, 2019.

Technical corrections

27. Line 110. Why does period have a – afterwards rather than a comma?

We agree that commas do as good a job here as the long dashes and have changed the text accordingly.

References

Browning, K.A., Hardman, M.E., Harrold, T.W. and Pardoe, C.W., 1973. The structure of rain bands within a mid-latitude depression. Quarterly Journal of the Royal Meteorological Society, 99(420), pp.215-231.

Browning, K.A., Roberts, N.M. and Illingworth, A.J., 1997. Mesoscale analysis of the activation of a cold front during cyclogenesis. Quarterly Journal of the Royal Meteorological Society, 123(544), pp.2349-2374.

Attribution of precipitation to cyclones and fronts over Europe in a kilometer-scale regional climate simulation

Stefan Rüdisühli[1], Michael Sprenger[1], David Leutwyler[2], Christoph Schär[1], and Heini Wernli[1]

[1]Institute for Atmospheric and Climate Science, ETH Zurich, Switzerland
[2]Max Planck Institute for Meteorology, Hamburg, Germany

Correspondence: Stefan Rüdisühli (stefan.ruedisuehli@env.ethz.ch)

Abstract.

This study presents a detailed analysis of the climatological distribution of precipitation in relation to cyclones and fronts over Europe for the nine-year period 2000–2008. The analysis uses hourly output of a COSMO (Consortium for Small-scale Modeling) model simulation with 2.2 ~~km~~ km grid spacing and resolved deep convection. Cyclones and fronts are identified as two-dimensional features in 850 hPa geopotential, equivalent potential temperature, and wind fields, and subsequently tracked over time based on feature overlap and size. Thermal heat lows and local thermal fronts are removed based on track properties. This data set then serves to define seven mutually exclusive precipitation components: high-pressure (e.g., summer convection), cyclonic (near cyclone center), cold-frontal, warm-frontal, collocated (e.g., occlusion area), far-frontal, ~~high-pressure (e.g., summer convection),~~ and residual. The approach is illustrated with two case studies with contrasting precipitation characteristics. The climatological analysis for the nine-year period shows that frontal precipitation peaks in ~~winter and fall~~ fall and winter over the eastern North Atlantic~~and the Alps (>70%in winter), where~~ , with cold frontal precipitation ~~is also~~ also being crucial year-round near the Alps; cyclonic precipitation is largest over the North Atlantic (especially in summer~~with >40%~~) and in the northern Mediterranean (~~widespread >40%~~except in summer); high-pressure precipitation occurs almost exclusively over land and primarily in summer~~(widespread 30-60%, locally >80%)~~; and the residual contributions uniformly amount to about 20 % in all seasons. Considering heavy precipitation events (defined based on the local 99.9^{th} percentile) reveals that high-pressure precipitation dominates in summer over the continent~~(50–70%, locally >80%)~~; cold fronts produce much more heavy precipitation than warm fronts; and cyclones contribute substantially~~(50–70%)~~, especially in the Mediterranean in fall through spring and in Northern Europe in summer.

1 Introduction

Precipitation is one of the most central meteorological variables ~~. Therefore~~and, therefore, huge efforts have been invested in compiling regional and global precipitation climatologies from surface station measurements, remote-sensing data, and

combinations thereof (e.g., **?????**). Such climatologies, with typically monthly time resolution, serve to characterize the spatial patterns, seasonal cycle, and interannual variability of precipitation, and they are valuable for strategic decisions in different socio-economic sectors (e.g., water management, agriculture, hydropower generation). Long-term climatologies reveal large interannual variability and trends (e.g., **??**). Among the most important questions for future climate change is how a warmer climate will affect precipitation and its climatological distribution, seasonality, interannual variability, and the occurrence of extreme events. In the global mean, precipitation is expected to increase at a rate of 2 % per degree global-mean warming, but changes in short-term precipitation are likely to occur at much faster rates (**???**). In the last decade, huge progress has been made in realistically simulating the hydrological cycle with high-resolution climate models, including the spatial distribution of precipitation, its diurnal cycle, and the statistics of extreme events (e.g., **????????**). A major part of this progress is due to the step-change of simulating deep convection explicitly instead of using a parameterized representation. In their systematic comparison of climate model simulations with parameterized or explicit convection, **?** found that "Improvements [when using explicit convection] are evident mostly for climate statistics related to deep convection, mountainous regions, or extreme events."

An important aspect of understanding the precipitation climatology and, eventually, its sensitivity to climate change, is the linkage of precipitation to synoptic-scale weather systems. As outlined below, high-pressure systems, extratropical cyclones, fronts, orography, ~~high-pressure systems,~~ and their interactions contribute essentially to the formation of precipitation in the mid-latitudes, including extreme events related to deep convection. Research in this area has so far mainly followed two strands: (i) detailed investigations of specific high-impact precipitation events, their large-scale precursors ~~,~~ and mesoscale dynamics (e.g., **??????**); and (ii) global climatologies to quantify the relevance of cyclones, fronts, warm conveyor belts, and atmospheric rivers for total and/or extreme precipitation (e.g., **??????**). However, most climatological studies on the relationship between precipitation and synoptic weather systems are based on global reanalyses with a typical resolution of 100 km in space and 6 h in time. Such a resolution is clearly inadequate to capture phenomena like short-duration convective precipitation events or the complex interplay between fronts~~and steep topographyin producing~~ , steep topography, and precipitation. In addition, a distinction between convective and stratiform precipitation is challenging at such resolutions. While some models distinguish stratiform (explicit) and convective (parameterized) precipitation, the convective fraction strongly depends on the model (**?**, see their Fig. 3).

This study aims at filling these gaps by using high-resolution data to quantify the co-occurrence of precipitation and a set of weather systems over Europe in the present-day climate. ~~A~~ To this end, kilometer-scale climate simulations with explicit convection ~~provides~~ provide the ideal data base to perform such a methodologically and computationally demanding analysis. The following paragraphs provide a concise summary of the link between precipitation and frontal cyclones, summarize how this link has been quantified in previous studies, explain in more detail the usefulness of high-resolution climate simulations for studying this link on climatological timescales, and outline the specific objectives of this study.

Explaining the surface precipitation pattern has been a major aspect of the Norwegian cyclone model, introduced almost a century ago by **?**. They realized that most cyclones are associated with a warm front, which slopes gently forward with height and produces widespread, rather uniform precipitation of moderate intensity; followed by a cold front, which is steeper,

slopes rearward with height, and produces much more intense but less widespread precipitation (**?**). In the time since, several aspects of the original Norwegian model have been revised, and new features of extratropical cyclones have been introduced. On the large scale, an important addition has been the concept of characteristic airstreams, among them the warm conveyor belt, a warm and moist airstream that ascends along and ahead of the cold front and overruns the warm front, all the while producing large amounts of precipitation (**??**). Recent studies suggest that embedded convection can occur within the mostly stratiform cloud band formed by this airstream, leading to intense peaks in surface precipitation (**???**). Observational studies have also revealed complex mesoscale structures in and around the large-scale frontal precipitation areas. In the vicinity of the warm front, there may be about 50 ~~km wide,~~ km-wide intense warm-frontal rainbands (e.g., **??**). In the comparatively dry warm sector, isolated mesoscale precipitation areas ~~about~~ can occur; 10 km to 100 km in size~~can occur, which~~ , they are triggered by large-scale ascent and topography (**?**). ~~In the warm sector ahead of the cold front, precipitation from low-level orographic clouds can be strongly enhanced via the seeder-feeder process (?) by precipitation from aloft (??).~~ Along the cold front, mesoscale systems such as rainbands, squall lines, or thunderstorms can develop (**???**). In the cold sector behind a frontal cyclone, where cold advection and large-scale subsidence prevail, ~~shallow convective~~ shallow-convective shower cells typically produce intermittent precipitation of light to moderate intensity over a large area (e.g., **??**). This very brief summary clearly indicates the complex and rich mesoscale substructures of surface precipitation in extratropical cyclones. In addition, isolated deep convection and the formation of mesoscale convective systems also frequently occur within surface anticyclones and in situations with weak sea-level pressure gradients (e.g., **??**).

In the past, a variety of approaches have been used to quantify the occurrence of precipitation in cyclones and across fronts. For surface cyclones (and anticyclones), such an attribution is methodologically straightforward once they have been identified as two-dimensional features, for instance bounded by closed sea-level pressure contours (**?**). For fronts, such an attribution is less straightforward, because objective frontal identification can be difficult, and because fronts are typically identified as one-dimensional line objects. Classically, cross-frontal profiles of precipitation have been derived from station measurements for single events or as multi-annual composites of frontal passages, for instance in Berlin (**?**), Munich (**?**), and Helsinki (**?**). While such studies can capture the full natural variability of fronts at a certain location, it is difficult to generalize the results to other locations or to larger areas. Studying frontal precipitation climatologically over large areas requires gridded precipitation and temperature data~~along with~~ , automated front detection, and precipitation attribution. While such methods are in principle objective, choosing specific approaches and configurations involves many ultimately subjective choices. Lacking a universally accepted definition of fronts, it is not inherently clear how to identify them, and consequently, many different approaches exist, as discussed in detail by **?** and **?**. Another subjective choice is involved when attributing precipitation to a front within a certain distance, which might also depend on the resolution of the available data sets. For instance, **?** used a 5°-wide search box to attribute precipitation from a global measurement data set to fronts based on reanalysis fields on a coarse 2.5° grid. Also using reanalysis data, **?** first identified coherent precipitation objects and then attributed them to objectively identified cyclones and fronts based on overlap criteria.

This brief summary of ~~attribution approaches of~~ approaches to attribute precipitation to weather systems ~~, –~~ in particular fronts ~~, –~~ together with the mesoscale characteristics discussed above, illustrate a range of challenges: (i) Precipitation data

with high spatial and temporal resolution is essential to capture (embedded) convective events (ideally, 1 km and 1 h); (ii) high-resolution fields of (equivalent) potential temperature are required to accurately determine the position and evolution of fronts, in particular near orography; (iii) data with homogeneous quality must be available, ideally ~~at a continental scale~~ on a continental-scale domain and for at least a decade, in order to compile robust climatologies; and (iv) computationally efficient algorithms need to be developed to objectively identify fronts, cyclones, and ~~high-pressure systems~~anticyclones, as well as for automatic attribution of precipitation to these features. Currently, purely observational data sets hardly meet requirements (i–iii), although hourly gridded precipitation data recently became available from satellites (**?**). Reanalyses ~~may~~ might become an option, given that global fields from ~~the~~ ERA5 reanalysis (**?**) by the European Centre for Medium-Range Weather Forecasts (ECMWF) are available with hourly resolution on a 30 km grid, and ~~that~~ regional reanalyses, e.g., the German product COSMO-REA2 (**?**), exist with a 2 km grid spacing and high temporal resolution. Currently, however, such high-resolution regional analyses are limited to sub-continental domains, which makes it difficult to meaningfully identify cyclones and fronts (as discussed below). For now, the best option is to use data from continental-scale decadal climate simulations performed with a high-resolution model with explicit deep convection. Recently, such simulations became feasible thanks to a major investment in porting the COSMO (Consortium for Small-scale Modeling) weather and climate prediction model to GPU architectures (**???**). For this study, output from a European-scale COSMO simulation for a 10-year present-day climate period ~~,~~ – with 2.2 km grid spacing, explicit convection, and hourly output ~~,~~ – will be used to perform a detailed climatological attribution of simulated precipitation to relevant weather systems. The main advantages of this approach are ~~:~~ the consistency between the high-resolution data set of surface precipitation and those of all the other meteorological fields required for identifying weather systems; the ~~size of the computational domain capable of representing for a decade the evolution of these systems over Western Europe , the eastern North Atlantic, and the Mediterranean~~ comparatively large domain covering most of Europe (see Fig. 1); and the explicit treatment of deep convection, leading to an improved realism in representing the diurnal cycle of summertime precipitation and extreme events. The ~~representation of frontal precipitation in the Kyrill storm was assessed in previous studies (**??**), which concluded that performing simulations at convection-resolving resolution yields a more physically consistent representation of frontal precipitation. The~~ drawback of using climate model data is that, despite using reanalyses as lateral boundary conditions, individual precipitation systems in the interior of the domain may develop differently in the simulation compared to reality. Therefore, it does ~~generally~~ not allow for an accurate precipitation attribution for a specific event in the simulation period~~. Instead, it enables~~ ; instead, it leads to a detailed climatological analysis of the role of anticyclones, cyclones, and fronts for total and heavy precipitation in Europe, separately for each season. The main objectives of this study are to:

1. develop algorithms that can meaningfully and efficiently identify and track ~~cyclones, fronts, and~~ surface high-pressure systems, cyclones, and fronts in the kilometer-scale climate simulation, and robustly attribute hourly precipitation to these weather systems;

2. quantify the contributions to total precipitation of cold fronts, warm fronts, cyclone centers, and high-pressure systems, and ~~to~~ investigate the geographical and seasonal variability of ~~these contributions~~this attribution; and

3. as above, but for heavy precipitation, defined annually and seasonally as hourly precipitation exceeding the respective grid-point-specific 99.9^{th} all-hour percentile.

In Sec. 2, we introduce the data set and the methodology; in Sec. 3, we demonstrate our approach with two case studies; in Sec. 4, we present climatological results from the precipitation attribution; and in Sec. 5, we summarize the main findings.

2 Data and Methods

2.1 Simulation and Field Preprocessing

We use hourly output from a ten-year regional climate simulation (1 January 1999 to 31 December 2008) with explicit deep convection over Europe, performed with a GPU-enabled prototype of the COSMO model (version 4.19) (**?**). A detailed description and evaluation of the simulation along with the detailed model setup ~~can be found in ?? and ?~~is found in **???**. We only analyze the nine-year period from 1 January 2000 to 31 December 2008 because not all fields necessary for our analysis have been archived during the first few months of the simulation. The domains of the nested COSMO simulations with 12 km ~~and~~ and 2.2 km grid spacing are shown in Fig. 1, together with the analysis domain of the high-resolution nest and the model topography~~of the 2.2 kmsimulation~~. The analysis domain corresponds to the full computational domain minus ~~104 grid points (∼ 228.8 km) in each direction (those~~ the grid points that are affected by the boundary relaxation~~). The orography differs between the driving ERA-Interim data, the 12 kmsimulation, and the 2.2 kmsimulation. While in response we expect significant local differences in precipitation, for instance in the vicinity of the Alps (see ? for a more thorough discussion), the larger-scale differences are expected to be small and locally confined, as the simulation is still sufficiently constrained by the lateral boundary conditions~~. The COSMO simulation in the high-resolution nest, with a horizontal grid spacing of 2.2 km, has been performed on a $1536 \times 1536 \times 60$ grid. At the boundaries, it is driven by one-way nesting ~~by~~ in a COSMO simulation with a horizontal grid spacing of 12 km on a $355 \times 355 \times 60$ grid. The domain of this coarser simulation is approximately 500 km larger in every direction than that of the nested simulation. In the 12 km simulation, deep convection is parameterized with an adapted version of the Tiedtke mass flux scheme (**?**). The coarser COSMO simulation ~~, in turn ,~~ in turn is driven at the boundaries by global ECMWF Interim Reanalysis data available on a 1° grid ~~every 6 h~~ (**?**).

The high spatial resolution of the 2.2 km simulation presents some challenges for the objective identification of cyclones and fronts. While the domain of the 2.2 km simulation is large given its horizontal resolution, it is still relatively small with respect to these synoptic systems. This causes problems, for instance, when a large-scale North Atlantic cyclone enters the domain from the west, because our algorithm cannot robustly identify cyclone features close to the boundaries, especially if their center (defined as the local pressure minimum) has yet to enter the domain. In addition, the high horizontal resolution can present challenges for our frontal identification algorithm, which is based on horizontal gradients (see below). From a technical perspective, the driving 12 km simulation thus at first glance appears to be more suitable to identify cyclones and fronts. However, this ignores that ~~the fronts and cyclones are influenced by~~ small-scale processes resolved in the nested 2.2 km simulation influence the fronts and cyclones, as evidenced by their sometimes substantially different development in the two

simulations in terms of their exact size and location – especially far ~~downstream of~~ from the lateral boundaries ~~, such as~~ and in the Mediterranean. These differences make it impossible to simply base the feature identification on the 12 km simulation. ~~Instead, in~~ In order to exploit the advantages of both simulations, the 2.2 km and 12 km data are merged in the following three-step procedure:

1. Interpolate the 2.2 km fields ~~to the part of~~ onto the 12 km grid~~covered by the domain of the~~ . This retains the exact position and extent of the cyclones and fronts in the 2.2 km simulation ~~.~~

2. ~~In the interior of the domain at a distance of at least 50 coarse grid points (~ 600 km) from the boundary~~ while increasing the signal-to-noise ratio to the level of the ~~2.2~~12 km ~~domain (dashed box in Fig. 1), use these fields from~~ simulation.

3. Paste these into the ~~2.2~~12 km ~~simulation.~~

4. ~~Outside the~~ fields to obtain hybrids comprised of 2.2 km ~~domain, use the fields from the~~ simulation data in the center and 12 km simulation data beyond the boundaries of the inner nest.

5. ~~In-between (between the semi-bold and the dashed box in Fig. 1), blend the fields with $f = 0.1/(1 + \exp(-0.8 \times (10\,x - 5)))$, where x increases linearly from 0.0at the inner boundary of the blending zone to~~ Introduce a blending zone along the boundaries in the inner domain with a smooth transition from the ~~1.0~~2.2 km ~~at the outer boundary and f increases logistically in the same range, corresponding to the fraction of~~ data to the 12 km data. It extends 50 coarse grid points (~ 60 km) into the inner domain and is based on the logistic function $1/(1 + \exp -k \times x)$ with $k = 0.8$.

The resulting hybrid fields ~~possess the bigger domain and lower noise level~~ reside on the grid of the 12 km simulation ~~, which allows for a more robust feature identification over the analysis domain , especially close to the boundaries such as over the North Atlantic. At the same time, they are~~ and thus benefit from its large domain and relatively low noise level, while being meteorologically consistent with the 2.2 km simulation within the analysis domain in the inner nest. We use ~~the hybrid fields on the 12 kmgrid~~ them to identify cyclones (Sec. 2.2) ~~,~~ and fronts (Sec. 2.3)~~, and high-pressure areas~~ . Before conducting the precipitation attribution analysis (Sec. ~~2.4~~2.5), ~~and then use the resulting feature masks at~~ however, the features are interpolated back onto the original 2.2 km ~~for the precipitation attribution analysis (Sec. 2.5)~~grid.

2.2 Cyclones

The cyclone identification is based on the approach by **?**, who identified cyclones as two-dimensional features defined by closed sea level pressure contours around local minima~~;~~ , along with the refinements by **?** ~~;~~ and the extension to multi-center cyclones by **?**. For this study, the algorithm had to be adapted for limited-area domains. Additionally, ~~in contrast to **?** and **?**,~~ tracking over time is based on the full ~~two-dimensional~~ extent of the two-dimensional features (see Appendix A) ~~rather than~~ as opposed to only their center ~~positions~~points as in the original tracking scheme by **?** and **?**. As input fields, instead of sea level pressure, we use geopotential (Φ) at 850 hPa for the sake of consistency with the fronts identified at that level. Seasonal feature and track frequency composites are provided in the supplementary material (Figs. S.S1 ~~and~~ and S2)

The Φ field is first smoothed with a Gaussian filter ~~with a standard deviation $\sigma = 7$~~to eliminate spurious extrema on the high-resolution grid. In order to avoid artifacts, we exclude areas within two grid points (~ 24 km) from the boundaries. Contours are then identified at an interval of $1\,\mathrm{m^2\,s^{-2}}$. Following **?** and **?**, the outermost enclosing contour around each local minimum is detected by stepping through ~~all~~ its enclosing contours until ~~:~~ there is no further enclosing contour~~;~~, or until the next contour also encloses either a local maximum ~~; or the next contour also encloses~~ or a fourth local minimum – the last criterion being a consequence of allowing up to three local minima per cyclone following **?**. Two depth criteria are applied to eliminate spurious minima, whereby the depth of a cyclone feature corresponds to the difference in Φ between ~~its lowest~~ a local minimum and its outermost enclosing contour~~(as determined by the criteria above)~~. First, multi-center cyclone features that are too shallow are split into multiple single- or double-center cyclone features, using the same approach (based on the relative depth of saddle points between minima) and thresholds as **?**. Second, very shallow cyclone features with a total depth below $1\,\mathrm{m^2\,s^{-2}}$ are discarded.

The approaches by **?**, **?**, and **?** were developed for global data sets. Limited-area domains introduce an additional complication because it is impossible to determine whether contours that leave the domain are open or closed, ~~and/~~or whether they contain additional minima or maxima outside the domain. It is not obvious how to best deal with such boundary-crossing contours~~; there is a range of possible assumptions one may make~~. At one ~~end~~ extreme is the assumption that all boundary-crossing contours are open, which ~~immediately stops the growth of any cyclone feature that reaches the domain boundary. While this choice is save, it~~ inhibits further growth of cyclone features at the boundaries and thus severely limits the size of cyclones in the vicinity of the boundaries~~, which has effects far into the domain. At the other end is the assumption~~ . The assumption at the other extreme is that all boundary-crossing contours are closed, which~~allows the cyclone features to continue growing uninhibited by the boundary. However, this often has the opposite effect, resulting in~~ , however, allows for unreasonably large cyclone features in certain situations with a relatively flat pressure distribution. We opt for a compromise by allowing ~~up to 20%of the~~ one in five contours of a feature ~~to be boundary crossing. For example, if 16closed contours are identified around a pressure minimum before the boundary is reached, then at most four additional boundary-crossing contours can be added before the~~ (20 %~~threshold is reached at four out of twenty contours~~) to cross the boundary before halting further feature growth.

2.3 Fronts

The front identification approach is based on **?** and ~~involves multiple steps~~constitutes a multi-step procedure:

- compute fields of frontal strength and velocity;
- based on ~~these~~them, identify cold-frontal and warm-frontal areas as two-dimensional features;
- track these features over time; and
- categorize the resulting front tracks further as either synoptic or local.

~~The local fronts are then removed, as only the synoptic fronts are used in this study.~~ Seasonal feature and track frequency composites are provided in the supplementary material (Figs. S1 and S2).

Fronts are characterized by strong horizontal contrasts in low-level temperature and humidity, which ~~makes~~ qualifies equivalent potential temperature θ_e at 850 hPa as a suitable field for ~~front~~ their detection (specifically, we use the modulus $|\nabla\theta_e|$ of the θ_e gradient~~)~~. **?** discuss this choice in detail and provide a historical context. Following the general approach proposed by **?**, the front identification method developed by **?** is based on applying the thermal front parameter (TFP) (**?**) to θ_e ~~,~~and using the cross-frontal wind component to distinguish between cold, warm, and quasi-stationary fronts.

Input fields are smoothed with the diffusive filter described by **?** with 160 repetitions. Further noise reduction is achieved by computing the gradient at each grid point across multiple unit grid distances using offsets of $(i \pm 4, j \pm 4)$ instead of $(i \pm 1, j \pm 1)$.

The frontal areas are derived from a thermal and a wind component:

- The thermal component is based on ~~$\theta_e|\nabla\theta_e|$~~ at 850 hPa~~. The θ_e field is first smoothed with the diffusive filter described by **?** with 25repetitions. Then~~ , from which a mask is derived ~~from its absolute gradient $|\nabla\theta_e|$~~by applying a minimum threshold~~, which~~ . The latter varies over the year to account for the strong seasonal cycle of humidity (and therefore of θ_e) ~~that leads~~ leading to substantially lower cross-frontal θ_e gradients in winter than in summer, and thus far fewer winter than summer fronts for a given threshold (**?**). A ~~$|\nabla\theta_e|$~~threshold value is defined in the middle of each month (Table 1) and linearly interpolated to each hour in-between.

- The wind component is based on frontal velocity v_f at 850 hPa:

$$v_f = \boldsymbol{v} \cdot \frac{\nabla\,(\mathrm{TFP})}{|\nabla\,(\mathrm{TFP})|} \tag{1}$$

where $\boldsymbol{v}$ is the horizontal wind vector and TFP denotes the thermal front parameter, defined as:

$$\mathrm{TFP} = -\nabla\,|\nabla\theta_e| \cdot \frac{\nabla\theta_e}{|\nabla\theta_e|} \tag{2}$$

A mask is derived with $|v_f| \geq 1\,\mathrm{m\,s^{-1}}$.

The frontal areas correspond to the overlap between the thermal and the wind component masks. The sign of v_f determines whether an area is classified as cold-frontal ($v_f \geq 1\,\mathrm{m s^{-1}}$) or warm-frontal ($v_f \leq -1\,\mathrm{m s^{-1}}$).

In a next step, the frontal features are tracked over time using the tool described in Appendix A. Cold-frontal and warm-frontal features are tracked separately. A minimum lifetime criterion of 24 h is applied to discard short-lived fronts. The resulting front tracks are then grouped into synoptic and local fronts based on track properties. ~~Synoptic fronts are generally larger and more mobile (i.e., less stationary) than local fronts , which are~~ Local fronts – largely produced by differential heating along topography and coasts – are generally smaller and more stationary than synoptic fronts. These properties can be expressed by a pair of criteria (on which we have settled after extensive manual testing):

- The *typical feature size* of a track is calculated by first combining, at each time step, the sizes of all features that belong to the track; and then calculating the median of these total sizes over all time steps. Front tracks are ~~only considered synoptic if the typical feature size is at least~~ considered local if the *typical feature size* does not exceed 1000 km^2.

– The *stationarity* of a track is determined as ~~the typical feature size divided by the~~ its total footprint area (defined by all grid points that belong to the tracked front at any time) divided by the *typical feature size*. Front tracks are ~~only considered synoptic if the stationarity is below~~ considered local if the *stationarity* does not exceed ~~0.167~~6.0.

All tracks fulfilling one or both criteria are considered ~~synoptic~~ local fronts, and thus ~~both large and mobile~~small and/or stationary. All remaining tracks are considered ~~local~~ synoptic fronts, and thus ~~small and /or stationary. Only synoptic fronts are used for the precipitation attribution analysis, while local fronts are removed~~both large and non-stationary.

2.4 High-Pressure Areas

Precipitation not only occurs near cyclones and fronts, but also in areas of weak synoptic forcing ~~that are~~ typically characterized by relatively high pressure ~~and~~ or by a flat pressure ~~distribution~~distributions, for example with diurnal summer convection over the continent. ~~When attributing precipitation only to cyclones and fronts, such precipitation would not be captured, but instead be part of the residual. Our original method without~~ We explicitly identify such high-pressure areas ~~, however, often misclassified diurnal summer convection as front-related (specifically *far-frontal*, as defined in Sec. 2.5). To prevent this, we first exclude precipitation in such areas characterized by high-pressure and a flat pressure distribution (henceforth simply called *high-pressure areas*), which we identify based on the~~ based on geopotential Φ and its gradient $\nabla\Phi$ at 850 hPa. Seasonal ~~frequency fields of the identified high-pressure areas~~ feature frequency composites are provided in the supplementary material (Fig. S1).

~~Computing the high-pressure areas (at 850 hPa) involves the following steps: Smooth the~~ The Φ field ~~using~~ is first smoothed with a Gaussian filter~~with a standard deviation $\sigma = 3$. Then compute a Φmask covering areas with high pressure, based on~~. A mask is derived by applying a minimum threshold ~~which~~ that varies over the year to account for the seasonal cycle in Φ. ~~The thresholdat a given time step is derived by linear interpolation from the mid-monthly values listed in~~ Analogous to the seasonally varying frontal threshold, the Φ threshold values are defined in the middle of each month (Table 2~~. Smooth the Φfield again using a Gaussian filter with a standard deviation $\sigma = 20$, then compute~~) and linearly interpolated to each hour in-between. Then, $\nabla\Phi$ ~~, whereby the gradient at each grid point is computedacross multiple unit grid distances using offsets of $(i \pm 10, j \pm 10)$, corresponding to $\pm 120\,\mathrm{km}$ in our hybrid 12 kmfields. Then compute a $\nabla\Phi$mask covering areas with a weak pressure gradient, based on~~ is computed, and the resulting field is smoothed again. A second mask is derived by applying a constant maximum threshold of $0.02\,\mathrm{m\,s^{-2}}$ ~~.~~ to $\nabla\Phi$. The high-pressure area corresponds to the overlap area of the Φ and $\nabla\Phi$ masks. All threshold values have been determined subjectively based on ~~extensive manual evaluation of multiple years of data~~thorough manual testing.

2.5 Front-Cyclone-Relative Components

In order to ~~attribute~~ associate precipitation to fronts and cyclones, we decompose the domain at each time step into seven so-called ~~*front-cyclone-relative*~~ front-cyclone-relative components, as illustrated in Fig. 2. They are mutually exclusive~~and defined~~

~~in the following order, where~~ , with each grid point ~~is~~ assigned to the first component ~~the criteria of which it fulfils~~for which it fulfills the criteria, and defined in the following order:

1. The **high-pressure** component comprises all grid points within a high-pressure area mask ~~,~~(regardless of the presence of ~~any~~ fronts or cyclones). Its purpose is to capture precipitation in areas of weak synoptic forcing such as diurnal summer convection over the continent. Applying this criterion first ~~, before all others,~~ prevents spurious front features ~~– frequent~~ that frequently occur in the Mediterranean in summer ~~–~~ from capturing diurnal summer convection precipitation as far-frontal.

2. The **cyclonic** component comprises all remaining grid points within a cyclone mask, regardless of the presence of ~~any~~ fronts. Its purpose is to capture precipitation produced ~~close to~~ near the center of cyclones.

3. The **cold-frontal** component comprises all remaining grid points within 300 km of a cold-frontal feature, but farther than 300 km from ~~any~~ a warm-frontal feature. Its purpose is to capture all precipitation produced close to cold fronts but in relative isolation from ~~the influence of~~ warm fronts and cyclone centers.

4. The **warm-frontal** component is analogous to the cold-frontal, but for warm fronts.

5. The **collocated** component comprises all remaining grid points within 300 km of both a cold-frontal and a warm-frontal feature. Its purpose is to capture precipitation simultaneously influenced by cold and warm fronts ~~, but~~ away from cyclone centers~~: ,~~ for instance, ~~areas near a~~ in areas of frontal fracture or frontal occlusion. In addition, it also occasionally captures strong warm conveyor belts, ~~because their eastern boundary~~ the eastern boundaries of which can be associated with a band of very high θ_e that is identified as a warm front ~~located within 300 km~~just ahead of the cold front.

6. The **far-frontal** component comprises all remaining grid points within 300–600 km of a front of either type. No distinction is made between ~~cold and warm fronts~~ the front type in order to keep the number of groups reasonably small. Its purpose is to capture precipitation more remotely related to ~~yet still influenced by~~ fronts.

7. The **residual** component comprises all remaining grid points. Its purpose is to capture precipitation that our approach cannot attribute to a specific weather system. Under the assumption that the other six components capture the major sources of precipitation, we expect the residual contributions to be comparatively small.

The thresholds that define the near-frontal (300 km) and far-frontal (600 km) components have been chosen subjectively based on our best judgment while studying a ~~wide~~ range of cases.

3 Case Studies

In order to illustrate our approach, we present two case studies ~~: one of a winter and one~~ of a summer ~~cyclone.~~

3.1 Winter Cyclone Lancelot

Winter storm Lancelot (?) affected Europe during 19–21 January 2007in the wake of well-known winter storm Kyrill (see ? for an animation based on the same simulation that includes both storms).

3.0.1 Development

At 00 UTC 20 January 2007(Fig. 5 a) the cyclone center approaches Ireland, accompanied by a warm front extending southeastward into the North Sea and Central Europe and a cold front extending southwestward across the British Isles into the North Atlantic. A large area of precipitation associated with the warm front extends over the North Sea to the rear of the cyclone center. A smaller band of precipitation accompanies the cold front, separated from the warm-frontal precipitation area by a dry gap region.

At 12 UTC 20 January 2007(Fig. 5 b), the cyclone center has almost completely crossed the North Sea and is approaching the southern tip of Norway. The cold front has been moving away from the cyclone center toward the southeast. It is oriented at a right angle to the warm front, forming a frontal T-bone typical of Shapiro-Keyser-type cyclones (Shapiro and Keyser, 1990). Along the cold front, oval-shaped precipitation cores are discernible, which are oriented at a slight clockwise angle relative to the front and separated by gap regions, reminiscent of a narrow cold-frontal rainband. In the cold sector behind the cyclone there is widespread patchy precipitation, some of it associated with a relatively shallow cyclone near the British Isles in a way reminiscent of secondary cold-frontal lines as described, for instance, by ?.

At 00 UTC 21 January 2007(Fig. 5 c), the cyclone center resides over the southern Scandinavian Peninsula. The warm front has moved across the southern Baltic Sea while still producing precipitation over an extended area. The cold front, by now far away from the cyclone center, has moved over continental Europe, extending from the North Atlantic near the northern tip of Iberia across France and Germany into Eastern Europe. It is oriented roughly parallel to the Alpine crest, which it steadily approaches. The eastern part of the cold front over Germany and Eastern Europe has started to disintegrate.

3.0.1 Precipitation Attribution

Figure 6shows the attribution to fronts and cyclones of the precipitation accumulated during the three days when cyclone Lancelot affected Europe. Total accumulated precipitation is distributed across most of the northern half of the domain, with a pronounced local maximum along the northern flank of the Alps (Fig. 6 a). In addition, local maxima occur over and west of Scotland, over southern Norway, and to a lesser degree over Denmark and along the Baltic coast. The Mediterranean is dry. Most components contribute at least some precipitation, with the exception of high-pressure areas (Fig. 6 e). A lot of precipitation is classified as frontal, with cold-frontal precipitation mainly north of the Alps (Fig. 6 b), warm-frontal precipitation covering an elongated region extending from the North Sea across Denmark into Poland (Fig. 6 c), and large amounts of collocated precipitation distributed in two distinct band-like regions farther south and north (Fig. 6 d). The precipitation maximum along the Alps is identified as primarily collocated – however, it largely predates the passage of Lancelot and is at least partially caused by remnants of Kyrill (the cyclonesystem immediately preceding Lancelot) as is evident from Fig. 5 and a

winter cyclone. ~~Also attributable is some cyclonic precipitation over southern Scandinavia and the Baltic (Fig. 6 f), along with some scattered far-frontal precipitation (Fig. 6 g). Residual precipitation is largely restricted to the northern part of the British Isles and the adjacent North Atlantic (Fig. 6 h). As Fig. 5 b, cindicate, post-frontal precipitation was largely responsible for the residual, partly organized in secondary frontal and cyclonic structures not identified as synoptic features.~~

3.1 Summer Cyclone Uriah

In late June 2007, cyclone Uriah (**?**) moved across the British Isles and the North Sea, accompanied by a strong cold front and a weak warm front.

3.1.1 Development

At 06 UTC 25 June 2007 (Fig. 3 a), the cold front is part of a baroclinic zone that extends from northeastern France southwestward to Gibraltar. The main precipitation areas are located just north of the cyclone center, as well as along and ahead of the cold front over France and Germany. East of the cyclone center, a weaker warm-frontal zone ~~(discernible from meteorological fields, not all shown)~~ extends into Eastern Europe, but ~~at this point~~ it is not yet recognized as a ~~frontal~~ front feature. Northwest of the cyclone center, cold and dry air is advected southward. The southern boundary of this cold zone constitutes a weakly precipitating cold front ~~that approaches~~ approaching the British Isles.

At 15 UTC 25 June 2007 (Fig. 3 b), the main cold front is gaining strength while moving over France and Germany. Its northern end has started to wrap around the cyclone center and produces substantial precipitation, while its southern end has reached the Alps, producing strong precipitation along the northern ~~Alpine flank~~ flank of the Alps. Behind the cold front, over France, many isolated cells produce fragmented precipitation of weak to moderate intensity. The warm front east of the cyclone, now detected as a feature, is much weaker than the cold front and ~~only produces some precipitation~~produces no precipitation, except close to the cold front, where occlusion may have commenced. ~~It has still not been identified as a feature by the algorithm.~~ The baroclinic zone southwest of the cyclone center has been fragmented while moving over Iberia and France. The minor cold front to the northwest of the cyclone center has reached Scotland and Ireland while falling dry.

At 06 UTC 26 June 2007 (Fig. 3 c), the main cold front has moved from Germany over Eastern Europe and southern Scandinavia. It is mostly oriented northwest-southeastward, except for its northern end, which is bent around the cyclone center. Precipitation is still substantial along most of the front. The precipitation band along its bent-back portion wraps almost completely around the cyclone center, much farther than the ~~corresponding~~ respective front feature, which suggests that ~~a part of the~~ not the whole front has been detected as a feature by our algorithm. The southern end of the cold front has been held back along the Alps, but orographic precipitation ~~there~~ has largely stopped. In the cold sector behind the front, over France and Germany, fragmented postfrontal precipitation is still prevalent. ~~By now, the weak warm front has been~~ The warm front is now detected as a ~~feature, but merely as a local front, which is not used for the precipitation attribution~~pair of thin warm-frontal features. Along most of its length, the warm front has been caught up by the cold front, suggesting occlusion. The baroclinic zone consisting of many small frontal fragments has crossed the Spanish and French coast into the Mediterranean. The minor

cold front over Great Britain at the boundary of the cold zone has stopped precipitating and is now followed by a pair of likewise dry warm fronts along the western border of the cold zone.

3.1.2 Precipitation Attribution

Figure 4 shows the attribution to fronts and cyclones of the ~~precipitation accumulated~~ accumulated precipitation during the four days when cyclone Uriah affected Europe. ~~In contrast to Lancelot (Sec. 3.2) – a fast-moving cyclone accompanied by a pronounced warm front and an extended cold front – Uriah constituted~~ We have characterized Uriah as a slow-moving cyclone accompanied by a pronounced cold front ~~but~~ and no discernible warm front. The precipitation attribution is entirely consistent with that~~characterization~~. Most ~~accumulated precipitation is concentrated~~ precipitation accumulated in a ring-shaped area centered on the Danish Straits, with maxima over the North Sea and southern Sweden (Fig. 4 a). The precipitation area extends over the British Isles and France to the west and southwest, and southward to the Alps; along the northern flank, precipitation amounts are locally enhanced. Southern Europe and the Mediterranean are entirely dry. Most precipitation is classified as either cyclonic (Fig. 4 f), mainly over the North Sea, southern Scandinavia, and the Baltic Sea; or cold-frontal, mainly over Germany and Poland near the Baltic coast and extending southwestward to the Alps (Fig. 4 a). While there is also some far-frontal and residual precipitation (Fig. 4 g, h), there is essentially no warm-frontal, collocated, or high-pressure precipitation (Fig. 4 c, d, e).

3.2 Winter Cyclone Lancelot

Winter storm Lancelot (**?**) affected Europe during 19–21 January 2007 in the wake of well-known winter storm Kyrill (see **?** for an animation based on the same simulation).

3.2.1 Development

At 00 UTC 20 January 2007 (Fig. 5 a) the cyclone center approaches Ireland, accompanied by a warm front extending southeastward into the North Sea and Central Europe, and a cold front extending southwestward across the British Isles into the North Atlantic. A large area of precipitation associated with the warm front extends over the North Sea to the rear of the cyclone center. A smaller band of precipitation accompanies the cold front, separated from the warm-frontal precipitation area by a dry gap region.

At 12 UTC 20 January 2007 (Fig. 5 b), the cyclone center has almost completely crossed the North Sea and is approaching the southern tip of Norway. The cold front has been moving away from the cyclone center toward the southeast. It is oriented at a right angle to the warm front, forming a frontal T-bone typical of Shapiro-Keyser-type cyclones (Shapiro and Keyser, 1990). The dry gap region between the fronts has disappeared. Along the cold front, oval-shaped precipitation cores are discernible, which are oriented at a slight clockwise angle relative to the front and separated by gap regions, reminiscent of a narrow cold-frontal rainband. In the cold sector behind the cyclone, there is widespread patchy precipitation, some of it associated with a relatively shallow cyclone near the British Isles.

At 00 UTC 21 January 2007 (Fig. 5 c), the cyclone center resides over the southern Scandinavian Peninsula. The warm front has moved across the southern Baltic Sea while still producing precipitation over an extended area. The cold front, by now far away from the cyclone center, has moved over continental Europe, extending from the Atlantic near the northern tip of Iberia across France and Germany into Eastern Europe. It is oriented roughly parallel to the Alpine crest, while steadily approaching it. The eastern part of the cold front over Germany and Eastern Europe has started to disintegrate.

3.2.2 Precipitation Attribution

Figure 6 shows the attribution to fronts and cyclones of the accumulated precipitation during the three days when cyclone Lancelot affected Europe. It moved faster and more zonally than cyclone Uriah and was accompanied by a large warm front and a long cold front, all of which is reflected in the precipitation contributions. Accumulated precipitation is distributed across most of the northern half of the domain, with a pronounced local maximum along the northern flank of the Alps (Fig. 6 a). In addition, local maxima occur over and west of Scotland, over southern Norway, and to a lesser degree over Denmark and along the Baltic coast. Like during the passage of cyclone Uriah, the Mediterranean is dry. Most components contribute some precipitation except, for high-pressure areas (Fig. 6 e). Much precipitation is classified as frontal, with cold-frontal precipitation mainly north of the Alps (Fig. 6 b), warm-frontal precipitation covering an elongated region extending from the North Sea across Denmark into Poland (Fig. 6 c), and large amounts of collocated precipitation organized in two distinct band-like regions farther south and north (Fig. 6 d). The precipitation maximum along the Alps is primarily collocated – however, that southern region of collocated precipitation largely predates the passage of Lancelot and is at least partially caused by remnants of Kyrill, the cyclone system immediately preceding Lancelot, as is evident in Fig. 5 a. Also attributable is some cyclonic precipitation over southern Scandinavia and the Baltic (Fig. 6 f), along with some scattered far-frontal precipitation (Fig. 6 g). Residual precipitation is largely restricted to the northern part of the British Isles and the adjacent North Atlantic (Fig. 6 h). As Fig. 5 b, c indicate, post-frontal precipitation was largely responsible for the residual, partly organized in secondary frontal and cyclonic structures not identified as synoptic features.

These case studies illustrate that our method is able to attribute precipitation to cyclones and fronts meaningfully and to capture the large case-to-case variability of the various contributions.

4 Climatology

In this section, the nine-year (2000-2008) climatology of precipitation and its link to the features in Fig. 2 are discussed. First, we consider the total precipitation in Sec. 4.1, whereby the annual and seasonal climatologies are discussed separately. Then, we focus on heavy precipitation in Sec. 4.2.

4.1 Total Precipitation

The main results of the total precipitation attribution are shown in Fig. 7 for absolute annual-mean amounts, Fig. 8 for absolute seasonal-mean amounts, and Fig. 9 for relative seasonal-mean contributions. In the annual mean, the ~~amounts of total~~

precipitation total precipitation amounts are generally larger in the northern part of the domain than in the Mediterranean. The largest amounts, however, occur over modest to high topography, especially the Alps, the Dinaric Alps, the Norwegian Alps, the Scottish Highlands, and the Pyrenees. In the North Atlantic, the precipitation amounts decrease from north/northwest toward south/southeast. With respect to the front-cyclone-relative contributions, several interesting features are discernible: (i) cold-frontal precipitation amounts are largest over the Alps and still large to the north/northwest thereof, but rather small in the Mediterranean and the Baltic Sea; (ii) large warm-frontal amounts are found over the North Atlantic and (to a lesser degree) over Central Europe, but almost none in they are also almost absent over the Mediterranean; (iii) cyclonic precipitation is relatively rather uniformly distributed across the domain with peak values in the North Atlantic, over the British Islesand , Northern Scandinavia, and in the Mediterranean the Mediterranean, which makes it the only component that contributes substantially to substantially contributes to the Mediterranean precipitation; (iv) the amounts of high-pressure precipitation amounts are large along a continental band extending from the Pyrenees to the Alps and the Dinaric Alps, with another a further band extending along the Apennines; and (v) the residual precipitation (i.e., the amounts that cannot be attributed to any front-cyclone-relative component), are relatively evenly distributed across rather evenly distributed in the domain, with enhanced values only discernible over the Alps and the Norwegian Alps.

The discussion so far has ignored the fact that there are significant seasonal variations (Fig. 8). In winter, the total precipitation is shifted from the continental regions to the North Atlantic. In spring, the distribution is similar as in close to the annual mean, except for slightly below-average amounts in the North Atlantic, the Baltic, and the Mediterranean Sea;, and slightly more precipitation over the Alps, the Pyrenees, and the Dinaric Alps. In summer, the spatial distribution across the domain is the least uniform among all seasons: The Mediterranean Sea and the Iberian peninsula are almost completely dry; meanwhile, most of continental Europe receives more precipitation than on average; and the contrast between the large precipitation amounts over the Alps and the dryer surrounding areas more pronounced than in any other seasonis biggest by far. Furthermore, during summer, no peak amounts are discernible over the Pyrenees and the Dinaric Alps, quite in contrast to spring and fall. Finally, the precipitation in fall is similarly distributed as in the annual mean, except for larger precipitation amounts in the North Atlantic relative to continental Europe. Peaks amounts in fall occur over the Alps, the Norwegian Alps, the Pyrenees, the Dinaric Alps, and the Scottish Highlands, as they do in the annual mean.

Like for In the same way as the amounts and geographical distribution of total precipitation precipitation exhibit a distinct seasonal dependence, seasonal variations can also be expected for the front-cyclone-relative components. Physically, this isof course , of course, based on the seasonal cycle of the considered weather features (cold and warm fronts, cyclones, high-pressure areas). For instance, it is well known that Alpine lee cyclones form preferentially during spring and fall in the Gulf of Genoa (e.g., **?**), or that North Atlantic cyclones with their accompanying attendant cold and warm fronts affect continental Europe more often in winter than in summer (e.g., **?**). Seasonal variations in the relative front-cyclone precipitation amounts must, therefore, be expected and interpreted with respect to the corresponding shifts in the weather features. In the supplementary material, we provide seasonal climatologies of fronts, cyclones, and high-pressure areas (Figs. S1 and S2) along with the occurrence and wet-hour frequencies of the front-cyclone-relative components (Figs. S3–S6). Here, we restrict the discussion to a few selected select seasonal effects on the relative precipitation amounts: (i) Cold-frontal The cold-frontal precipitation is

more uniformly distributed across the domain in winter and fall than in spring and summer, whereby in summer, cold-frontal precipitation is mostly restricted to the continent, specifically Western, Eastern, and Northern Europe; (ii) warm-frontal winter precipitation is similarly distributed as the annual mean – peak values over the North Atlantic and the British Isles, and somewhat smaller values over Central Europe – whereas summer warm-frontal precipitation is nearly non-existent over the continent; (iii) ~~the amounts of~~ cyclonic winter precipitation amounts are below the annual ~~mean~~ average over continental Europe and the North Atlantic, but above-average in the Mediterranean, especially in the Adriatic and Tyrrhenian Seas and over the Apennines, in contrast to summer with nearly no cyclonic precipitation over the Mediterranean Sea; and (iv) high-pressure precipitation dominates in summer over much of Western and Southeastern Europe, whereas ~~it~~ this component is completely missing during winter and only weakly discernible in spring and fall. This short list, of course, can only provide a glimpse on the many local seasonal effects. Furthermore, as mentioned before, we did not show and describe the seasonality of the collocated and far-frontal components, which, however, can be found in the supplementary material (Figs. S3–S6).

Instead of analyzing in greater detail the ~~absolute~~ *absolute* precipitation amounts and how they can be attributed to the front-cyclone-relative components, we now consider the ~~relative~~ *relative* contributions by addressing the questions what percentage of the total precipitation can be attributed to a ~~the main components of a~~ front-cyclone system, and what percentage is attributable to either the high-pressure or residual components. The results are shown in Fig. 9, split according to season and for the components: frontal~~(~~, i.e., ~~cold-frontal,~~ cold- or warm-frontal~~, or collocated), cyclonic ,~~ ; cyclonic and far-frontal~~,~~ ; high-pressure~~,~~ ; and residual. ~~Several noteworthy signals are discernible~~There are several signals discernible that are noteworthy. During winter~~and fall~~, a substantial percentage ($> 70\,\%$) of the total precipitation ~~occurs close~~ can be attributed to fronts over the North Atlantic~~and Central Europe(up to >70%in winter, about 60%in fall), and~~ , Central Europe, and (to a lesser degree~~the Mediterranean (up to >50%). Far-frontal precipitation is neither as prevalent, nor as variable, with 10–20%in most areas year-round~~) the Mediterranean. Cyclonic and far-frontal percentages are largest in the Mediterranean, particularly in spring (regionally up to 50~~%~~ %). High-pressure percentages are negligible except for summer ~~,~~ when the contribution ~~exceeds 70%~~over the Iberian peninsula, mid- to southern Italy, and Sardinia/Corsica ~~. As expected~~becomes larger than 70 %. Of course, part of the total precipitation cannot be attributed to any of the components. The relative residual contributions are rather uniform, both in time and in space. In spring, they reach about 25~~%. Over~~ %. Especially in winter and fall, the residual percentages over Central Europe and the North Atlantic, including the British Isles, ~~the residual percentages~~ are still smaller~~at about~~ , about 10~~%, especially in winter and fall~~ %.

4.2 Heavy Precipitation

After the discussion of total precipitation in the previous section, we now shift our focus to heavy precipitation. It is defined as the amount of precipitation exceeding a local (i.e., grid-point-specific) threshold of hourly precipitation intensity, ~~corresponding~~ which corresponds to the 99.9^{th} all-hour percentile (i.e., including dry hours, as recommended by **?**), ~~or~~ corresponding to a return period of about 1.4 months. Separate thresholds are computed for annual and seasonal analyses, respectively.

The spatial distribution of the annual-mean heavy precipitation (Fig. 10 a) differs from ~~that or~~ total precipitation (Fig. 7) in that the former preferentially occurs over land~~, and in~~ ; and that heavy precipitation amounts in the Mediterranean are similar to

those over continental Europe and larger than those in the North Atlantic. While total precipitation exhibits the strongest spatial gradients from low to high topography, especially in the Alpine region, heavy precipitation shows a more pronounced land-sea-contrast, especially between the North Atlantic and continental Europe. Local maxima in ~~amounts of heavy precipitation~~ heavy precipitation amounts occur over high topography along the northern Mediterranean, specifically over the Alps, the Pyrenees, the Dinaric Alps along the Balkan coast, and the Apennines.

The front-cyclone-relative components of annual-mean heavy precipitation can be sorted into two groups: (i) cold-frontal, high-pressure, cyclonic, and residual precipitation (Fig. 10 b, e, f, h), which each contribute substantial amounts of heavy precipitation in specific areas; and (ii) warm-frontal, collocated, and far-frontal heavy precipitation contributions (Fig. 10 c, d, g), which are ~~much~~ substantially smaller and will therefore not be discussed any further. Some specific attribution results with respect to the first group are: (i) Cold-frontal heavy precipitation (Fig. 10 b) ~~occurs in large amounts~~ is large over and around the Alps, as well as along the Balkan and the northwestern Iberian coasts; (ii) high-pressure heavy precipitation (Fig. 10 e) is restricted to continental areas~~(~~, both Europe and North Africa~~)~~, and contributes by far the largest share ~~of~~ to heavy precipitation over land; (iii) cyclonic heavy precipitation (Fig. 10 f) resembles ~~cyclonic total~~ total cyclonic precipitation in its relatively even spatial distribution and only weak local enhancement over high topography, while contributing almost all heavy precipitation over the Mediterranean Sea and ~~,~~ to a lesser degree ~~,~~ in the North Atlantic and the North Sea; and (iv) ~~amounts of~~ residual heavy precipitation amounts (Fig. 10 h) tend to be larger over land than over sea and ~~to~~ increase toward Eastern Europe, albeit ~~–~~ in contrast to total precipitation ~~–~~ without any local enhancement over high topography.

Like total precipitation, heavy precipitation exhibits seasonal variations in both geographical distribution and front-cyclone-relative attribution. The clear separation into the two above-mentioned groups in the annual mean disappears~~at the seasonal level~~, which reflects the fact that different mechanisms are responsible for heavy precipitation in different seasons ~~, –~~ which is expected given the seasonality of the considered weather features (see supplementary material, Figs. S1 and S2). Heavy winter precipitation (Fig. 11 a) is more prevalent over sea than over land~~– in contrast~~, as opposed to the annual mean~~–~~, with the largest amounts over the Mediterranean ~~(–~~ and especially the Ionian ~~)–~~ Sea, as well as along the Iberian west coast. In spring, heavy precipitation (Fig. 11 a) exhibits a pronounced land-sea-contrast with large amounts distributed evenly across continental Europe and local maxima over the Alps and the ~~Tunisian Atlasmountains~~Tunesian Atlas. Compared with winter, this corresponds to pronounced a north- and landward shift of heavy precipitation in the southern part of the domain. No season experiences more heavy precipitation than summer (Fig. 11 a) ~~, the season~~ when the northward shift since winter ~~peaks. Amounts of heavy precipitation~~ reaches its peak. Heavy precipitation amounts are large over all of continental Europe except Iberia, with peaks over the Alps, and moderate further north over the British Isles, the Baltic, and the North Atlantic. Meanwhile, the Mediterranean Sea and southern Iberia are almost dry. The onset of fall is accompanied by a southward shift of heavy precipitation from continental Europe to the Mediterranean (Fig. 11 a). The spatial distribution is almost mirrored~~with respect to summer~~, with most heavy precipitation in the previously dry Mediterranean and Iberia while the land-sea-contrast along the rest of the North Atlantic coast completely disappears. Italy and the Balkan coast are the only extended regions where heavy precipitation is prevalent in both summer and fall. By far the largest ~~amounts of heavy precipitation~~ heavy precipitation

amounts occur along the coasts of France and Spain from the Gulf of Lion to the Balearic Sea, along with secondary hot spots ~~in~~ int the Tyrrhenian and Ionian Seas.

Heavy precipitation is attributable to different processes ~~in different seasons~~ from season to season (Fig. 11), ~~same~~ just as we have already shown for total precipitation (Fig. 8): (i) The main areas of heavy winter precipitation in the Ionian Sea and along the western Iberian coast originate primarily from, respectively, cyclones (Fig. 11 d)~~and~~ , and cold and warm fronts (especially ~~cold fronts~~the former; Fig. 11 b, c); (ii) similarly, the cyclonic component (Fig. 11 d) is the primary source of heavy precipitation in the Mediterranean in the other seasons, especially in fall, and over Northern Europe and the North Atlantic in summer; (iii) the widespread occurrence of heavy summer precipitation over the continent almost entirely coincides with high-pressure areas (Fig. 11 e), which on the other hand are completely irrelevant in winter; and (iv) while cold fronts (Fig. 11 b) steadily contribute heavy precipitation over the continent from spring through fall~~–~~, with peak contributions along the northwestern Mediterranean coast (Gulf of Lion, Gulf of Genoa) in fall~~–~~, warm fronts (Fig. 11 c) are mostly irrelevant for heavy precipitation.

~~Complementary to this discussion of the absolute front-cyclone-relative contributions to heavy precipitation, the relative contributions of a subset of the components are provided in the supplementary material (Fig. S07).~~

5 Conclusions

Hourly fields from a kilometer-scale regional climate simulation for present-day climate conditions over Europe, covering the nine-year period 2000–2008, have been used to perform a detailed climatological attribution of total and heavy precipitation to a set of synoptic weather systems: cyclones, cold and warm fronts, high-pressure areas (capturing diurnal summer convection), and derived categories (regions with collocated cold and warm fronts and far-frontal regions). To the best of our knowledge, this is so far the most detailed synoptic feature attribution exercise for European precipitation, which led to important findings related to both methodological and meteorological aspects. First, the attribution has been applied to two storms passing over Europe: the ~~winter cyclone Lancelot~~ summer cyclone Uriah (~~19–21~~24–26 ~~January~~ June 2007), and the ~~summer cyclone Uriah~~ winter cyclone Lancelot (~~24–26~~19–21 ~~June~~ January 2007). Based on these two case studies, and further refined in the 2000-2008 climatological analysis, the methodological key aspects can be summarized as follows:

- Although fairly established algorithms existed for automatically identifying cyclones and fronts in comparatively coarse reanalysis and global climate simulation data, their application required great efforts in testing and adjusting for use with kilometer-scale simulation output (e.g., by increasing spatial smoothing and by introducing additional criteria). These efforts can hardly be automated, and the finally used thresholds are not universal, i.e., they would need further adjustment if considering a different region, climate model, or resolution. The final setup of our algorithms should not be regarded as perfect, but rather pragmatically as one out of potentially several meaningful options.

- A large model domain is required in order to meaningfully identify frontal cyclones, in particular in the North Atlantic storm track region. Although~~–~~, compared with previous kilometer-scale climate simulations~~–~~, our simulation was performed on a huge domain, it was essential to perform the identification of cyclones and fronts on the even larger

domain of the driving coarser model~~(using hybrid fields based on both simulations)~~. Only with this spatial extension, the robust identification of North Atlantic cyclones and their sometimes elongated trailing fronts approaching Europe became possible.

- A particular challenge related to the ~~front~~ frontal identification is the choice of the equivalent potential temperature gradient threshold. If a constant threshold is used, a spuriously high number of fronts appear in summer, while a substantial number of fronts are missed in winter. We therefore introduced a seasonally varying gradient threshold, which led to a fairly constant number of identified fronts throughout the year. However, this clearly emphasizes the degree of subjectivity associated with the identification of fronts, which directly affects the attribution of precipitation to those fronts.

The meteorological results of the precipitation attribution show that different components are important in different geographical regions and in different seasons. When considering precipitation over the entire year, the most relevant weather systems are cold fronts near the Alps, warm fronts and cyclone centers in the North Atlantic and Western Europe, and cyclones in the Mediterranean, in particular near Italy and the Balkans. A substantial residual exists (about 20–30 %), indicating that our weather system categories do not encompass all precipitation-producing flow situations and that the attribution to the target systems is not perfect. Strong local enhancement occurs over high topography compared to the sourrounding flat areas, which is especially pronounced over the Alps and for cold-frontal precipitation. From a seasonal perspective, (i) cold fronts are important contributors in all seasons (especially over the continent), while warm fronts primarily contribute in winter and fall (especially over the North Atlantic); (ii) the largest cyclonic contributions shift from the Mediterranean in winter to Northern Europe in summer; and (iii) high-pressure precipitation is confined to summer over the continent, with pronounced local enhancement over the Alps. Focusing only on heavy-precipitation events reveals substantial differences to total precipitation: (i) Rather than over high-topography, heavy precipitation is particularly enhanced over land compared to sea; (ii) cold fronts also contribute substantially to heavy precipitation, whereas the relevance of warm fronts diminishes; (iii) cyclones are particularly important for heavy precipitation over the ocean; and (iv) the summertime high-pressure systems further gain in significance, in particular for continental summer convection.

The results can be summarized concisely for several distinct geographical regions. In particular, we focus on (i) the British Isles, (ii) Western Europe (excluding the Alps), (iii) the Alps, (iv) Southeastern Europe (comprising Italy, ~~Corsica~~Corse, and the Balkan coast), (v) the Iberian Peninsula, and (vi) the Mediterranean Sea. The mean precipitation amounts over the whole domain and each region for all front-cyclone-relative components in each season are shown in Fig. 12. Of course, this selection of geographical regions is not exhaustive, and could easily be extended to other regions based on the distribution maps in this study (Figs. 7 to 11) and ~~in~~ the supplementary material (Figs. S2–S6).

- **British Isles:** Cyclonic and frontal precipitation are important throughout the year, but there is also a clear seasonal cycle: The cold-frontal contributions are larger in winter and fall than in spring and summer; warm-frontal contributions – which are larger than for any other region – exhibit a similar but more pronounced seasonal cycle as cold-frontal; and while the cyclonic contributions are relatively weak in winter, they are substantial in spring, fall and particularly summer.

High-pressure precipitation plays no role for the British Isles. For heavy precipitation, the importance of warm fronts diminishes while that of cyclones further increases, and while cyclones experience a more pronounced seasonal cycle with a shift from winter to summer, the seasonality of cold fronts markedly decreases.

- **Western Europe:** Cold-frontal precipitation remains important and uniform in its amplitude in Western Europe throughout the year. By contrast, half the annual warm-frontal precipitation is contributed in winter ~~, but~~ and almost none in summer. The relevance of cyclones, by contrast, is lowest in winter and peaks in spring. High-pressure precipitation only substantially contributes in summer, but then more ~~so~~ than any other component. With respect to heavy precipitation, cold fronts remain the main contributors overall, but no single-season contribution over Western Europe compares to that of high-pressure areas in summer, which equals or exceeds the annual contributions of all components except cold fronts and cyclones.

- **Alps:** ~~They~~ The Alps stand out in many maps as a region with considerably enhanced ~~amounts of precipitation~~ precipitation amounts. In all seasons, cold-frontal precipitation contributes substantially to the total precipitation amounts, whereby this signal is particularly strong during spring. Warm-frontal precipitation, on the other hand, is substantially reduced compared to cold-frontal and mostly restricted to fall and winter. Cyclonic and high-pressure precipitation are of equally high overall importance, but while the former exhibits a comparatively weak seasonal cycle, high-pressure precipitation primarily occurs in summer. The residual is notably large over the Alps, especially in spring and summer. This changes in the heavy-precipitation limit, though, where summer high-pressure precipitation gains even more relevance, followed ~~,~~ in total annual amounts ~~,~~ by cold-frontal and cyclonic precipitation.

- **Southeastern Europe:** Similarly to the British Isles, cyclonic precipitation is of great importance to precipitation in Southeastern Europe, but warm-frontal precipitation is not. While the cold seasons are markedly influenced by cold fronts and cyclones, high-pressure systems are more important in summer – although not nearly as dominant as over the Alps. Heavy precipitation exhibits a similar attribution profile~~as total precipitation~~, except for large amounts of summer high-pressure precipitation, as observed in many regions.

- **Iberian Peninsula:** Summers are very dry, with hardly any precipitation except relatively small amounts of high-pressure precipitation. The other seasons are strongly influenced by cyclones (especially spring) and cold fronts (especially fall) ~~,~~ along with some warm-frontal influence. The fraction of unattributable precipitation is large compared with other regions, especially in spring. Heavy precipitation exhibits a very similar attribution profile ~~as total precipitation,~~ except for larger summer high-pressure contributions.

- **Mediterranean Sea:** Cyclonic contribution dominate in all seasons, although in summer, the Mediterranean receives almost no precipitation. Cold and warm fronts together contribute about the same total annual ~~amounts~~ amount of precipitation as cyclones, to which cold fronts contribute about twice as much as warm fronts. The cyclonic dominance is even more pronounced for heavy precipitation, especially in fall, when also the relative cold-frontal contributions increase compared ~~with~~ to total precipitation. High-pressure ~~heavy precipitation contributions are increased~~ contributions

increase in summer and fall for heavy precipitation. While all other regions experience more high-pressure precipitation in summer than in fall, the opposite is true in the Mediterranean Sea; this holds for both total and heavy precipitation.

Many of these results are plausible in the sense that they are consistent with meteorological expectations. We think that the particular value of this study are its objective approach, the quantitative results, and the high-resolution maps (Figs. 7 to 11), which ~~enable the discovery of~~ allow one to discover many interesting small-scale characteristics of European precipitation. It is interesting that this approach confirms the strongly opposing character of winter and summer precipitation, the former being very strongly associated with cyclones and fronts, and the latter predominantly ~~detected within~~ with high-pressure systems.

~~When summarizing these characteristics, it is important to mention another caveat: the comparatively short analysis period of nine years. While interannual variations in summer precipitation appear reasonably well covered with such simulations, variations in the North Atlantic oscillation suggest that longer integration periods are desirable or needed in order to adequately cover decadal variations of the winter season. A significant challenge of such analyses is the cost of storing high-resolution output of multi-decadal simulations. It is thus desirable to use an online analysis approach that performs the respective analysis while the simulation is running (??) instead of storing all the relevant output data. Such an online analysis tool can also be highly beneficial when extending the feature-based analyses in three dimensions, e.g., by defining fronts in 3D and/or by considering the vertical structure of clouds and microphysical processes.~~

There are different aspects that could be studied in forthcoming analyses. For instance, the results presented in this study show how the precipitation can be attributed to the front-cyclone-relative components under present-day climate conditions. It is, however, an open question whether the attribution to the components will be the same in the future climate. First steps to apply our approach to future climate simulations have been taken, and the results will be presented in a forthcoming publication. As an additional refinement, the frontal precipitation may be split into ~~pre-frontal, frontal, and~~ pre- or post-frontal components ~~. Such cross-frontal~~ or a component at the exact location of the front. Such front-relative precipitation profiles would be rather interesting and further refine our understanding of how precipitation is induced by ~~,~~ and thus attributable to ~~,~~ cyclone-frontal passages. Preliminary results in this direction look promising (**?**). ~~Finally, methods that separate precipitation types like convective and stratiform (e.g., **?**) could be combined with our feature-based attribution, which would enable a more in-depth characterization of the different front-cyclone-relative precipitation components.~~

Code availability. TEXT

Data availability. TEXT

Code and data availability. The data and analysis tools used in this study are available upon request.

Sample availability. TEXT

Video supplement. TEXT

Appendix A: Identification and Tracking Algorithm

Weather systems are explicitly identified as two-dimensional features comprised of adjacent grid points (including diagonal neighbors) and with characteristic properties such as size and center position. Tracking these features over time enables further characterization based on their time evolution, for instance by applying lifetime or stationarity criteria. Here, we provide a concise summary of our approach – for more details, the reader is referred to **?**[1].

The feature tracking algorithm is designed for data with high resolution in space and time. ~~Corresponding features at two consecutive time steps are determined as follows.~~ Whether a feature at one time step (the parent) corresponds to one or more features at the ~~other~~ next or previous time step (the children), depends on whether they exhibit sufficient overlap and similar total size. (This matching is done symmetrically both forward and backward in time, so the child features may well temporally precede their parent feature.) Based on these metrics, a tracking probability is computed and used to determine the features that correspond to each other. A connection between a parent and its child features constitutes a tracking event. Its type depends on the number of children and the temporal direction of the connection: continuation (one child), merging/splitting (multiple children, backward/forward), genesis/lysis (no children, forward/backward). The resulting feature tracks can contain an arbitrary number of merging and splitting events, and they are therefore in general not linear, but branched. This also implies that at any given time step, multiple features may belong to separate branches of the same track. The duration of a track is defined as the time difference between its earliest and the latest features, regardless of how the respective branches are connected in-between.

Author contributions. SR designed this study together with MS and HW. SR developed the analysis tools and produced the results. DL and CS contributed the output of the high-resolution simulation. SR did most of the writing, and all authors contributed to the discussion of the results and the final manuscript.

Competing interests. The authors declare that they have no conflict of interest.

[1]Note that in **?**, additional algorithmic components ~~– e.g.,~~ such as feature and track splitting ~~,~~ or topography filters ~~–~~ were described and applied to cyclones and fronts. Unless explicitly mentioned, they have not been applied in the present study.

Acknowledgements. The Swiss National Science Foundation supported this work under Sinergia Grant CRSII2_154486/1 crCLIM. Compute resources for the decade-long climate simulation were awarded through the Partnership for Advanced Computing in Europe (PRACE) on Piz Daint at the Swiss National Supercomputing Center (CSCS). Furthermore, we acknowledge Nicolas Piaget (formerly ETH Zurich) for technical support during the early stages of this work; Nikolina Ban (University of Innsbruck) for helpful discussions and comments; and Olivia Romppainen-Martius (University of Bern) for helpful feedback on an earlier version of this study. ~~We thank the two anonymous reviewers for their constructive feedback that helped us improve the manuscript in many places.~~

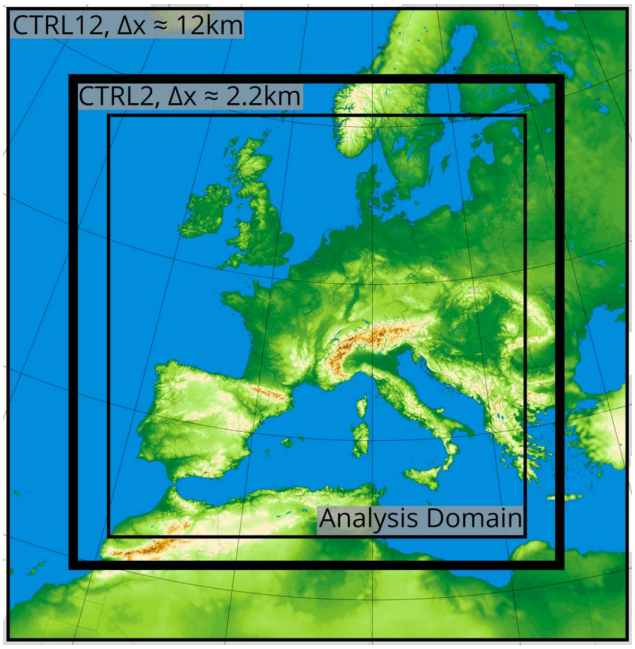

Figure 1. ~~Domain boundaries and model topography of the two~~ COSMO ~~simulations~~simulation domains and model topography. The ~~four~~ outermost black ~~boxes show, from large to small: (bold)~~ box denotes the ~~model~~ domain of the ~~driving~~ convection-parameterizing simulation with a ~~horizontal~~ grid spacing of 12 km ~~; (semi-bold)~~ and the bold box the ~~model~~ domain of the ~~nested~~ convection-resolving simulation with ~~a horizontal grid spacing of~~ 2.2 km ~~; (~~grid spacing. The innermost thin ~~)~~ box indicates the subdomain ~~of the 2.2 kmdomain on which the precipitation attribution analysis is performed; and (dashed) the inner boundary of the blending zone that is~~ used ~~during the computation of the hybrid fields on which the feature identification is based (see Sec. 2.1). The model topography inside (outside) the 2.2 kmdomain boundary is that of~~ in the ~~nested 2.2 km(driving 12 km) simulation~~analysis. (Figure and caption from **?**)

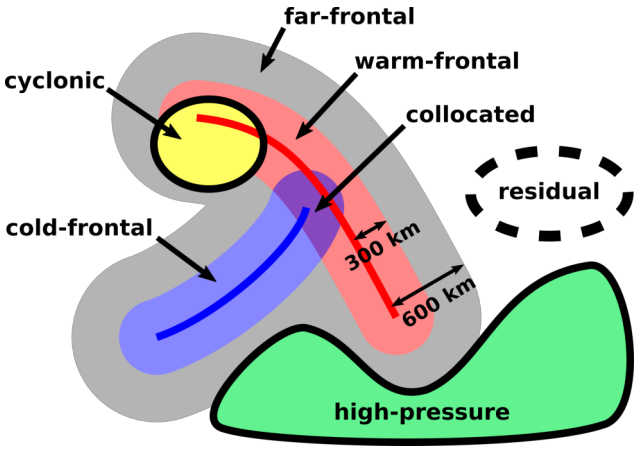

Figure 2. Schematic depiction of the seven front-cyclone-relative components ~~(as defined in Sec. 2.5):~~ high-pressure, cyclonic, cold-frontal, warm-frontal, collocated, far-frontal, and residual~~. Note that they are mutually exclusive and cover the whole domain~~, ~~i.e~~as defined in Sec.~~, at a given time step, each grid point is assigned to exactly one component~~ 2.5.

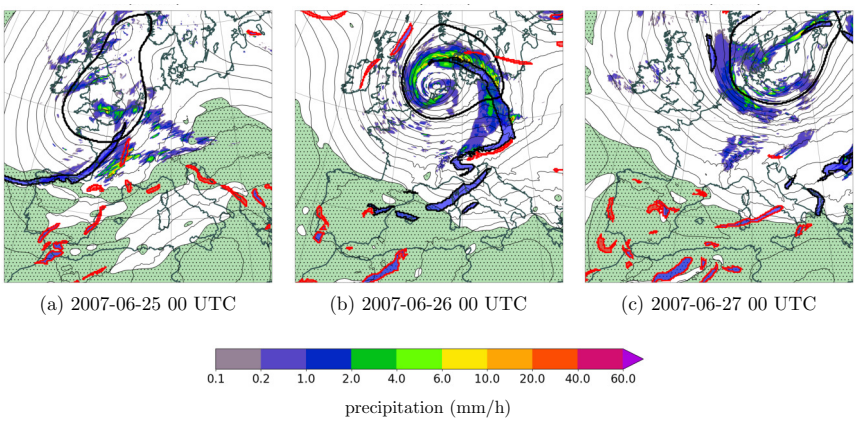

Figure 3. Development of cyclone ~~Lancelot~~ Uriah in ~~January~~ June 2007. ~~Thin~~ The thin black contours indicate ~~the~~ geopotential at 850 hPa~~, gray~~ ; the colored shading the surface precipitation~~, and green stippling~~ ; the ~~high-pressure areas. Bold~~ filled bold contours ~~represent~~ the outlines of ~~tracked~~ front features~~:~~ , with black/red outlines for synoptic~~cold and warm~~ /local fronts~~(blue~~ , and blue/red ~~), local~~ filling for cold/warm fronts; the unfilled bold contours the outlines of ~~either type (orange), cyclone features; and cyclones (black)~~the green stippling high-pressure features.

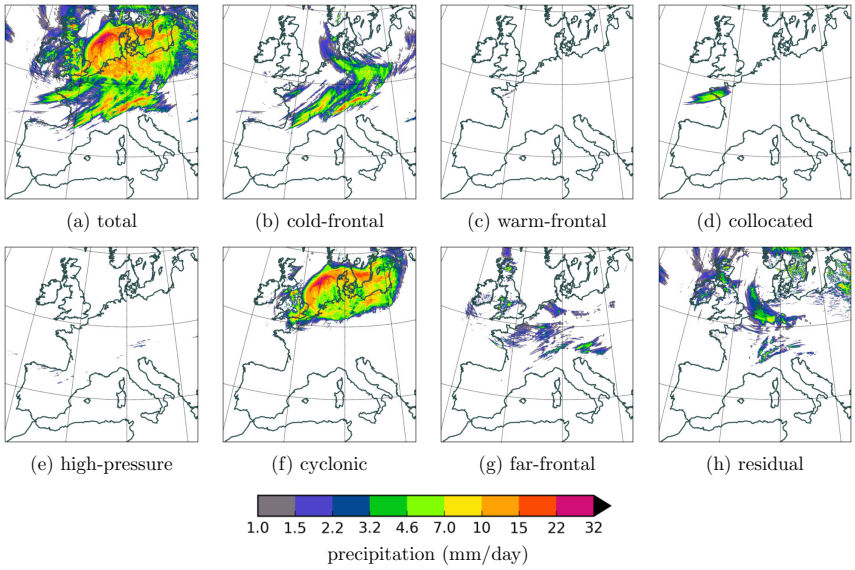

Figure 4. Front-cyclone-relative precipitation contributions to cyclone ~~Lancelot~~ Uriah during the period ~~19–21 January~~ 24–27 June 2007.

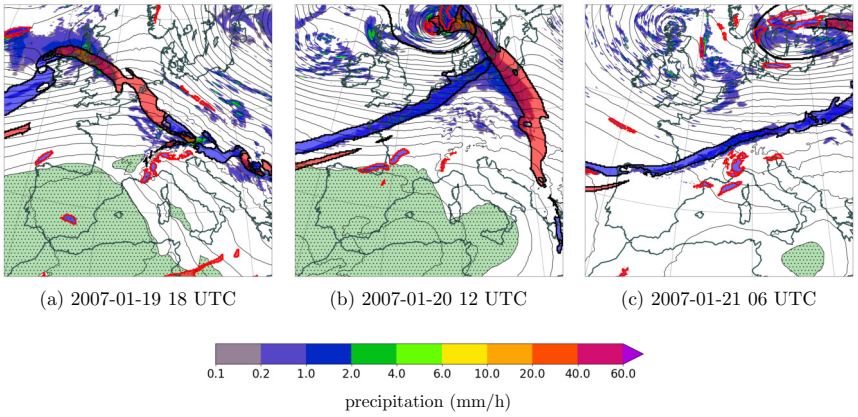

(a) 2007-01-19 18 UTC (b) 2007-01-20 12 UTC (c) 2007-01-21 06 UTC

Figure 5. As Fig. ~~5~~3, but for cyclone ~~Uriah~~ Lancelot in ~~June~~ January 2007. ~~Note that in (a), the precipitation along the cold front over northwestern Spain will be attributed to the high-pressure area instead, which takes precedence over fronts (see Sec. 2.5).~~

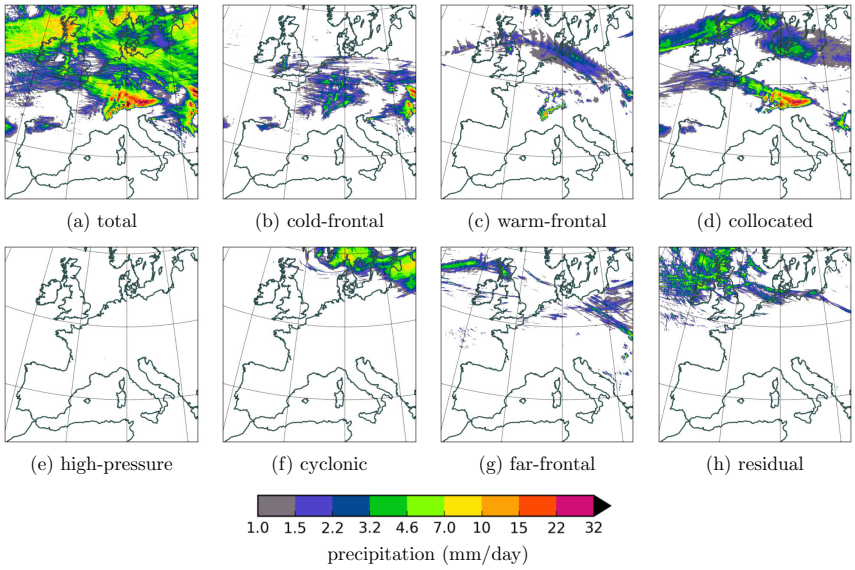

Figure 6. As Fig. ~~6~~4, but for cyclone ~~Uriah~~ Lancelot during the period ~~24–27 June~~ 19–21 January 2007.

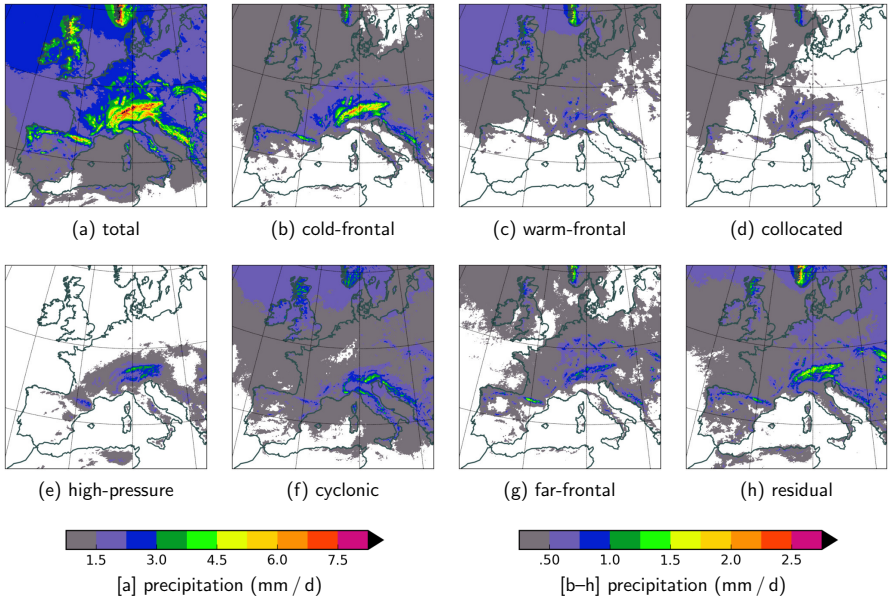

Figure 7. Mean daily precipitation during the nine-year period 2000–2008 (a) overall and (b–h) separated into seven front-cyclone-relative contributions.

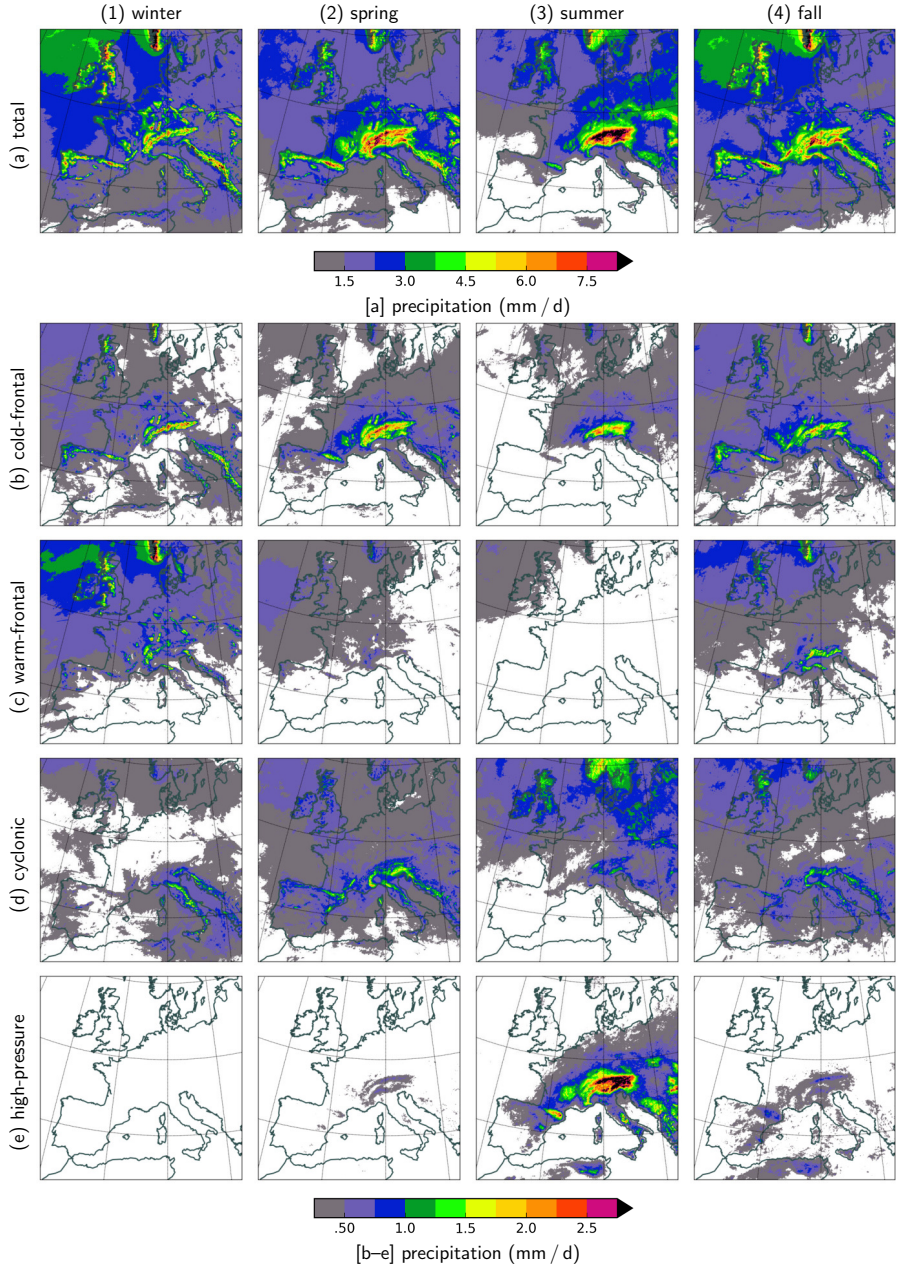

Figure 8. Mean daily precipitation during (1–4) each season of the nine-year period 2000–2008 (a) overall and (b–e) of ~~selected~~ select front-cyclone-relative contributions.

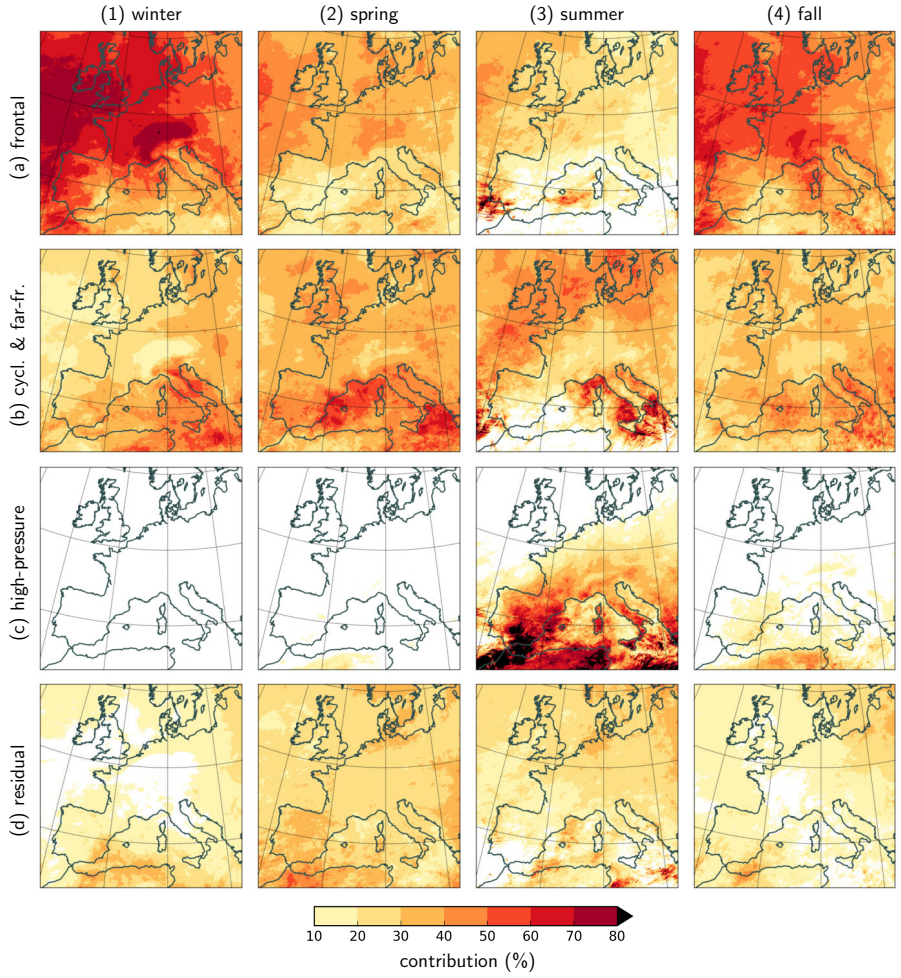

Figure 9. Relative precipitation contributions during (1–4) each season of the nine-year period 2000–2008 of front-cyclone-relative components: (a) sum of cold-frontal, warm-frontal, and collocated; (b) sum of cyclonic and far-frontal; (c) ~~cyclonic; (d)~~ high-pressure; and (~~e~~d) residual.

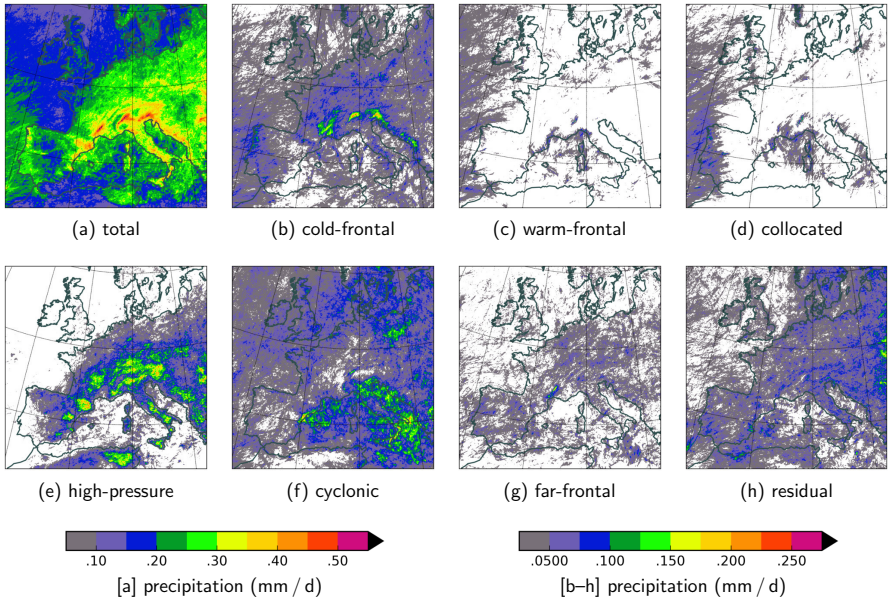

Figure 10. Like Fig. 7, but for annual heavy precipitation defined as the amount exceeding the local 99.9^{th} all-hour percentile of hourly precipitation intensity over the whole year.

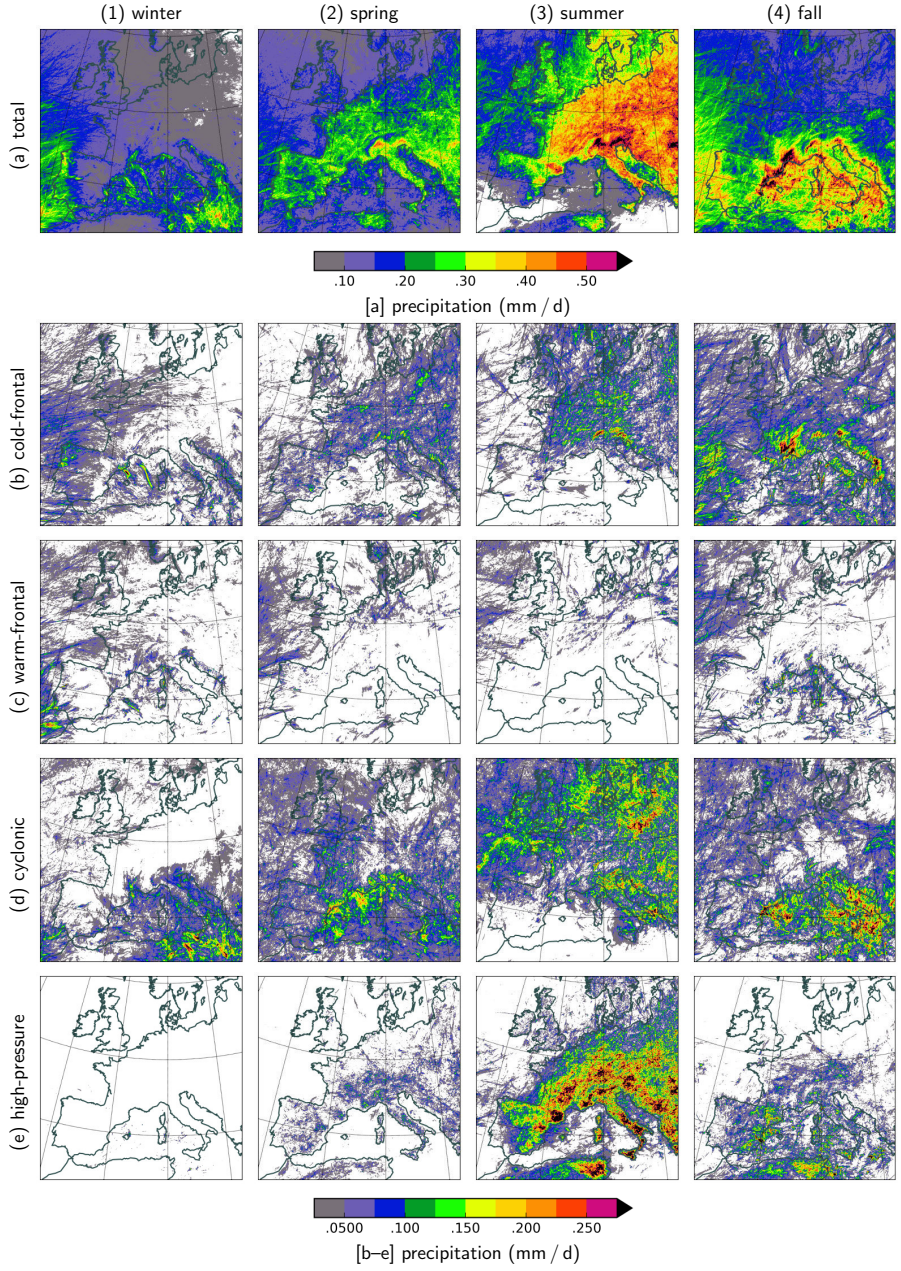

Figure 11. Like Fig. 8, but for seasonal heavy precipitation defined as the amount exceeding the local 99.9^{th} all-hour percentile of hourly precipitation intensity in a given season.

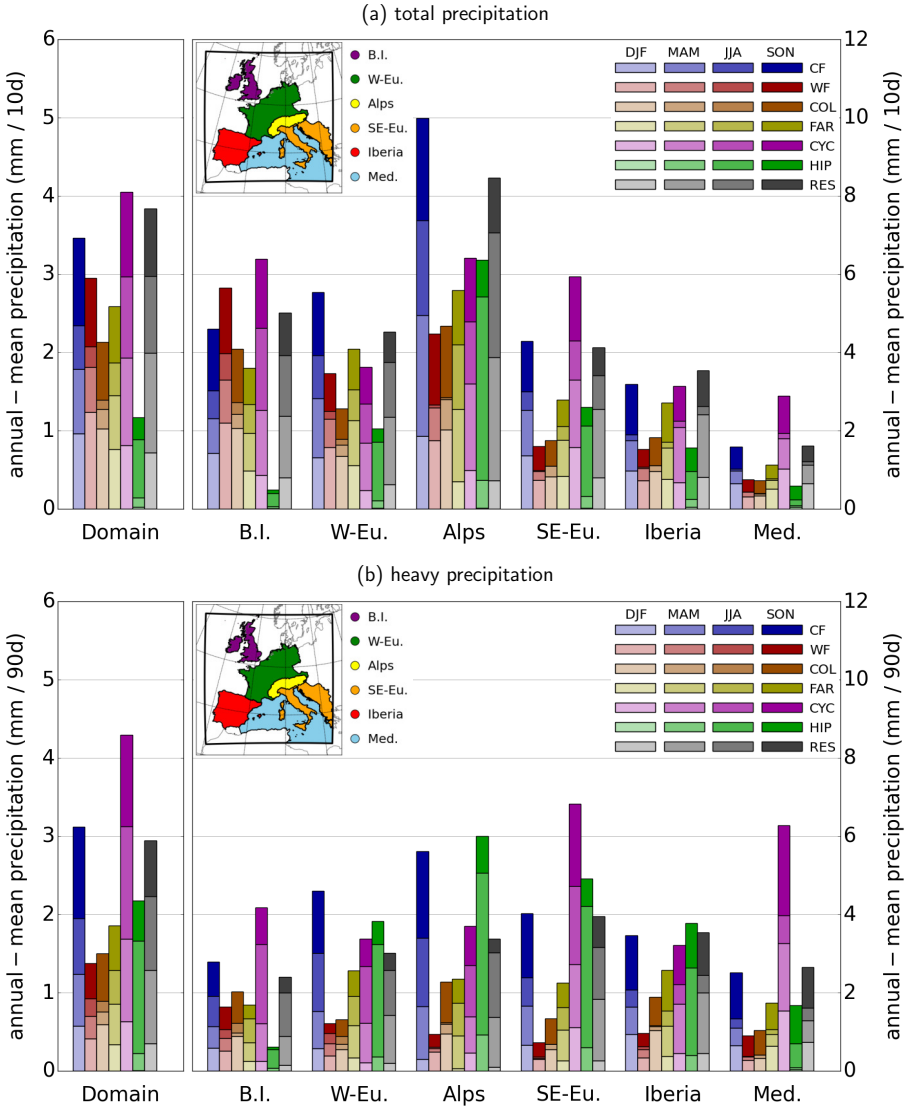

Figure 12. Mean (a) total and (b) heavy precipitation over the analysis domain and six ~~selected~~ select regions, as indicated in the map: British Isles, Western Europe, Alps, Southeastern Europe, Iberia, and the Mediterranean Sea. Heavy precipitation is defined as the amount of hourly precipitation above the local (grid-point specific) seasonal 99.9^{th} all-hour percentile. Each bar shows the annual-mean precipitation contribution of one front-cyclone-relative component (CF: cold-frontal; WF: warm-frontal; COL: collocated; FAR: far-frontal; CYC: cyclonic; HIP: high-pressure; RES: residual), with the four segments indicating the relative contribution of each season (DJF: winter; MAM: spring; JJA: summer; SON: fall). To obtain approximate absolute seasonal-mean amounts, multiply the height of a bar segment by four. Note that there is no relation between the colors of the bars and those of the regions on the map.

Table 1. Mid-monthly $|\nabla\theta_e|$ threshold values in K (100 km)$^{-1}$ to compute the thermal component of frontal areas, as described in Sec. 2.3.

Jan	Feb	Mar	Apr	May	Jun	Jul	Aug	Sep	Oct	Nov	Dec
4.0	4.0	5.0	6.0	7.0	8.0	8.0	8.0	7.0	6.0	5.0	4.0

Table 2. Mid-monthly Φ threshold values in $\mathrm{m}^2\mathrm{s}^{-2}$ to compute the Φ-component of high-pressure areas at 850 hPa, as described in Sec. 2.4.

Jan	Feb	Mar	Apr	May	Jun	Jul	Aug	Sep
~~15,500~~ 1550	~~15,500~~ 1550	~~15,250~~ 1525	~~15,000~~ 1500	~~14,750~~ 1475	~~14,500~~ 1450	~~14,500~~ 1450	~~14,500~~ 1450	~~14,750~~ 1475	~~15,~~

Supplement to *"Attribution of precipitation to cyclones and fronts over Europe in a kilometer-scale regional climate simulation"*

Stefan Rüdisühli[1], Michael Sprenger[1], David Leutwyler[2], Christoph Schär[1], and Heini Wernli[1]

[1]Institute for Atmospheric and Climate Science, ETH Zurich, Switzerland
[2]Max Planck Institute for Meteorology, Hamburg, Germany

Correspondence: Stefan Rüdisühli (stefan.ruedisuehli@env.ethz.ch)

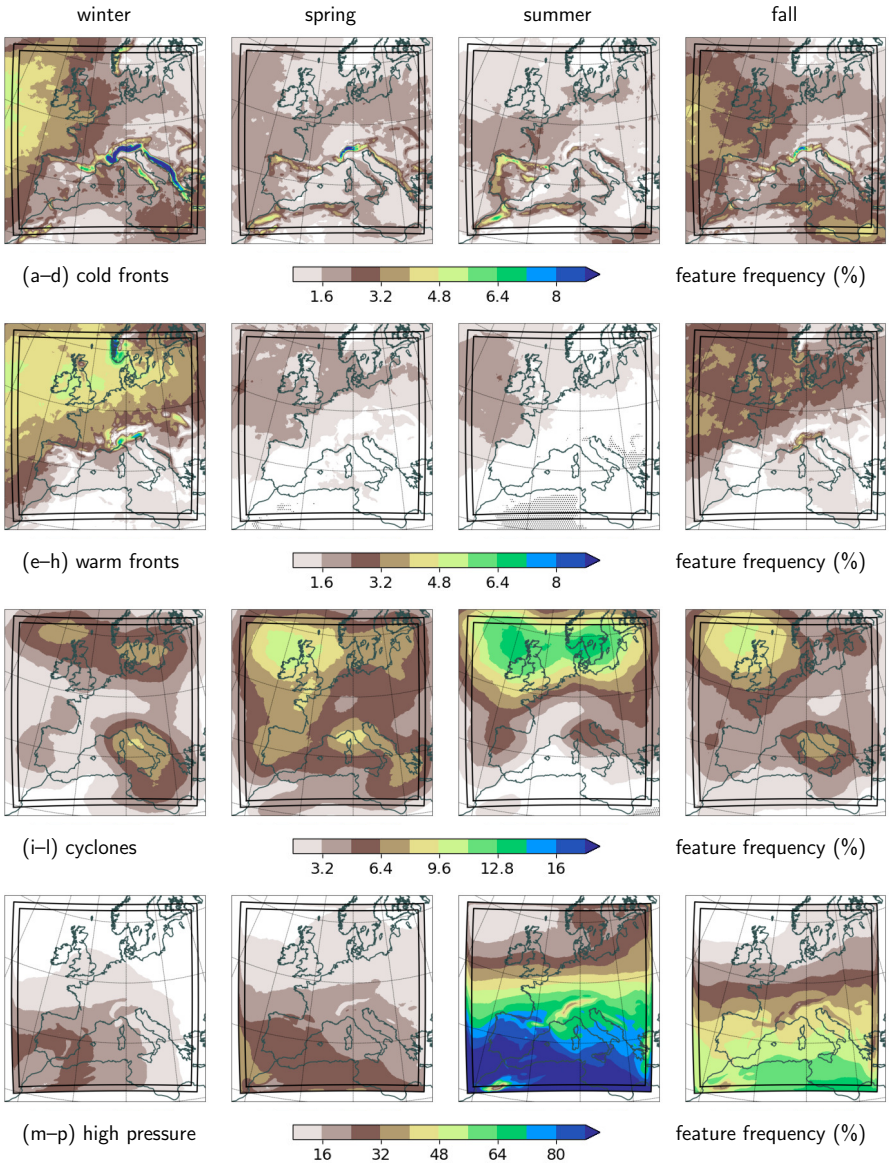

Figure S1. Feature frequencies of (a–d) cold fronts, (e–h) warm fronts, (i–l) cyclones, and (m–p) high-pressure areas during (left to right) winter, spring, summer, and fall 2000–2008. The outer black box shows the computational domain of the 2.2 km simulation, the inner box the analysis domain. The fields are computed by first reducing each feature in the respective time period to a binary mask field, and then averaging these binary fields to obtain the total feature frequency field.

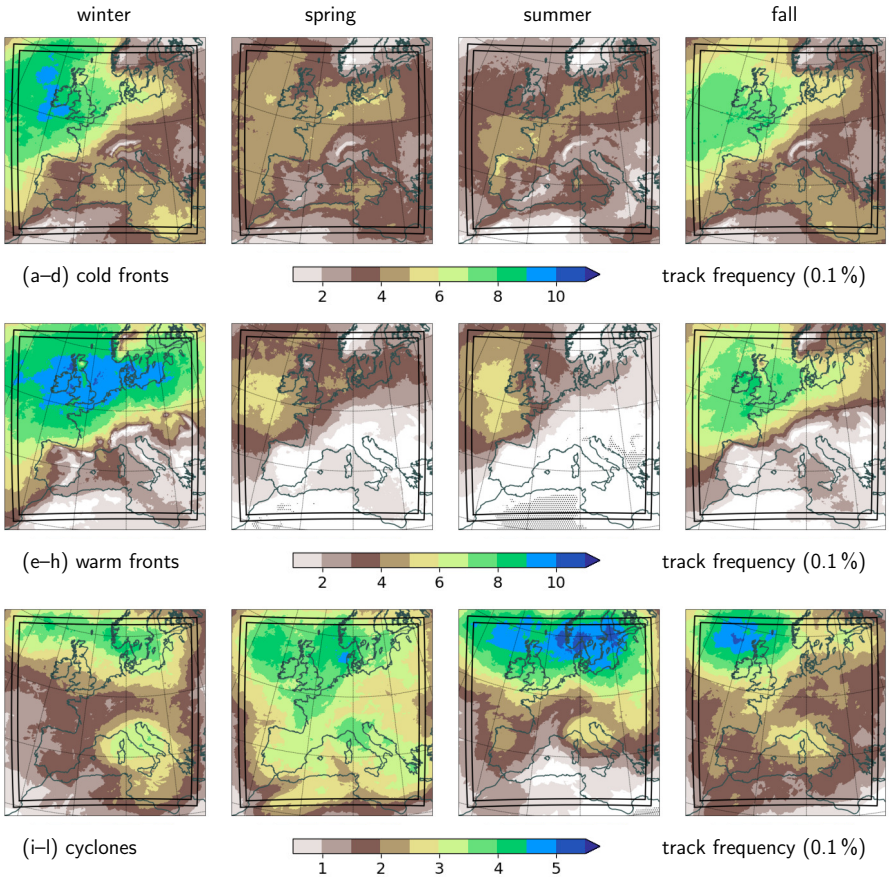

Figure S2. Track frequencies of (a–d) cold fronts, (e–h) warm fronts, and (i–l) cyclones during (left to right) winter, spring, summer, and fall 2000–2008. The outer black box shows the computational domain of the 2.2 km simulation, the inner box the analysis domain. The fields are computed by first reducing each track to a binary mask field comprised of all grid points affected by any feature belonging to the track in the respective time period, and then averaging these binary fields to obtain the total track frequency field.

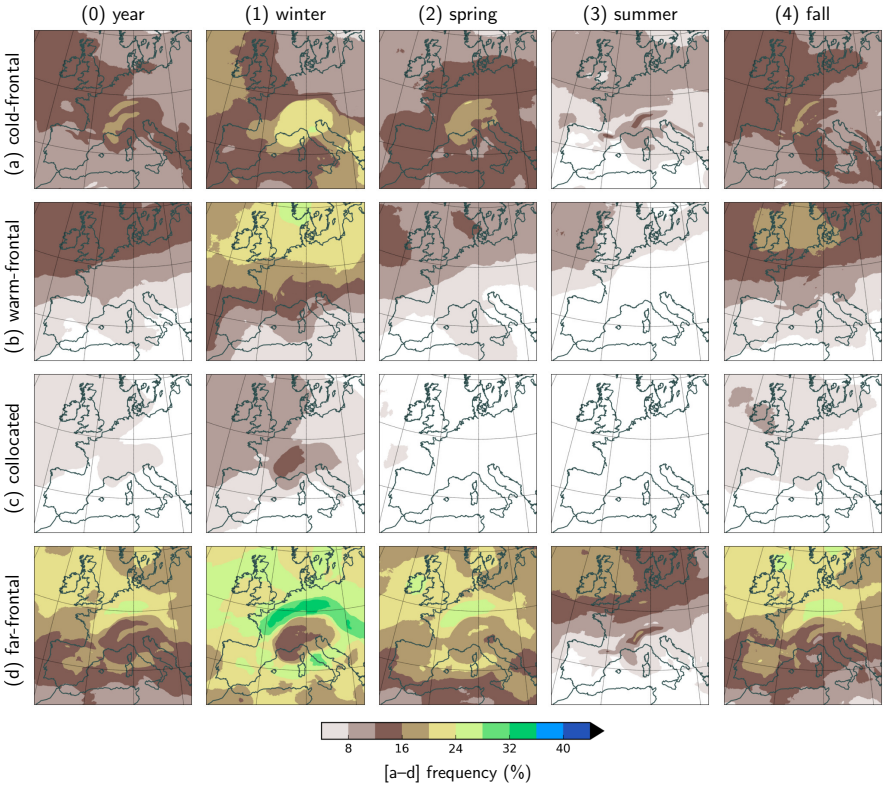

Figure S3. Frequencies of front-cyclone-relative ~~component masks~~ components during (0) the whole year, (1) winter (DJF), (2) spring (MAM), (3) summer (JJA), and (4) fall (SON) 2000–2008. ~~The masks are obtained at each time step by separating the domain into seven components as described in Sec. 2.5.~~ Shown are the (a) cold-frontal, (b) warm-frontal, (c) collocated, and (d) far-frontal components.

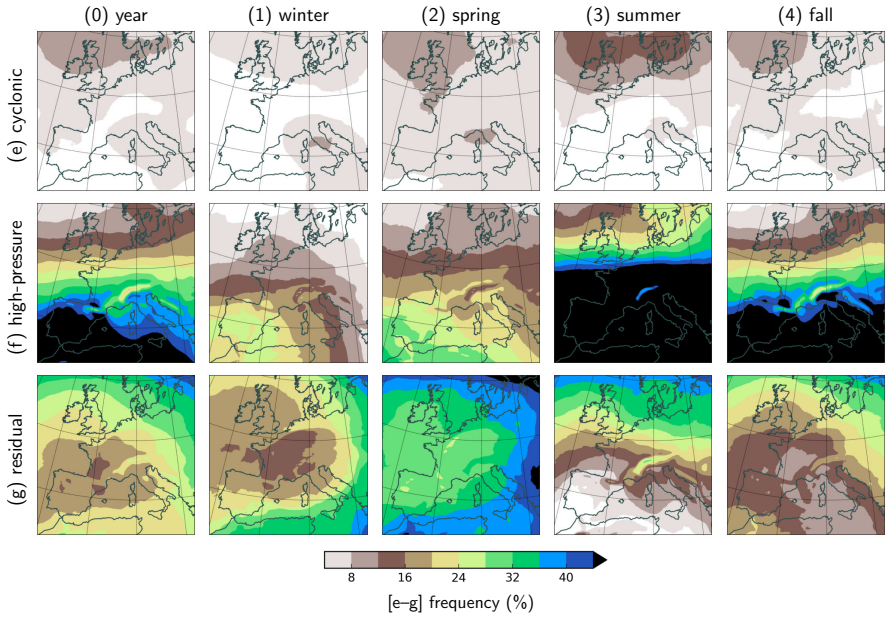

Figure S4. ~~Frequencies of front-cyclone-relative component masks as in~~ Like Fig. S3, but showing the frequencies of the (e) cyclonic, (f) high-pressure, and (g) residual components.

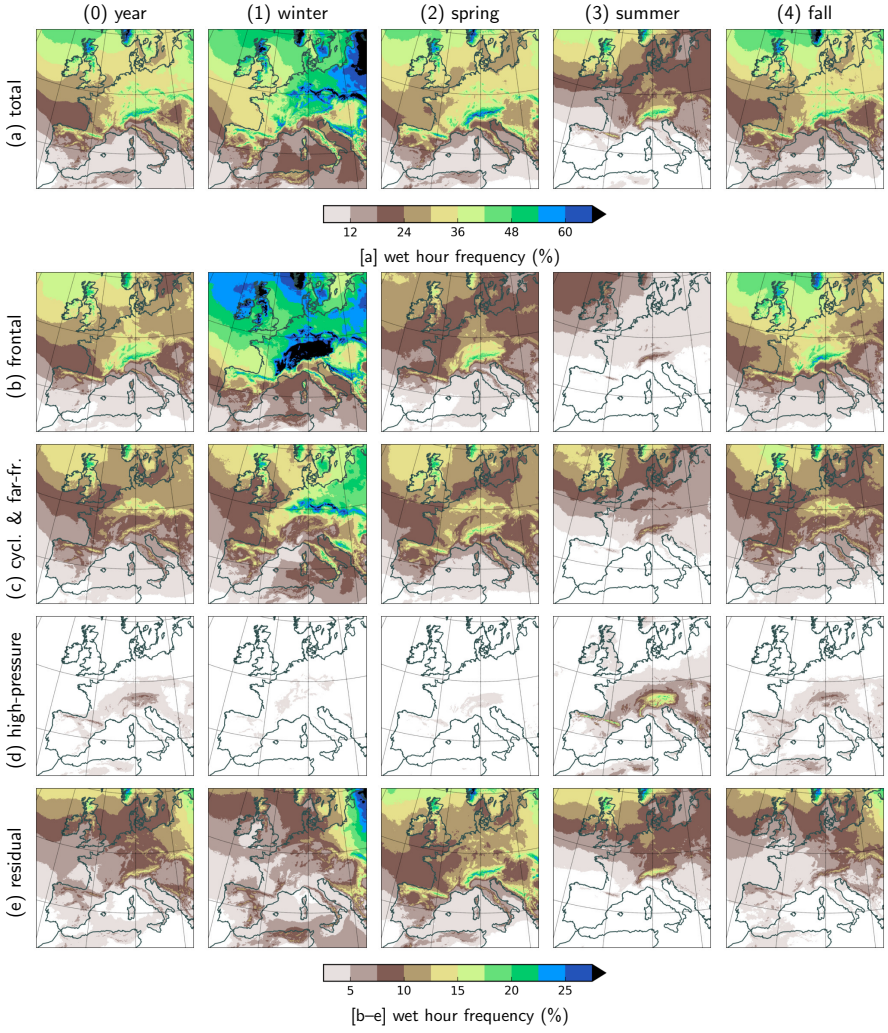

Figure S5. Wet-hour frequency during (0) the whole year, (1) winter (DJF), (2) spring (MAM), (3) summer (JJA), and (4) fall (SON) 2000–2008, (a) overall and (b–e) for sets of front-cyclone-relative components, specifically: (b) sum of cold-frontal, warm-frontal, and collocated; (c) sum of cyclonic and far-frontal; (d) high-pressure; and (e) residual.

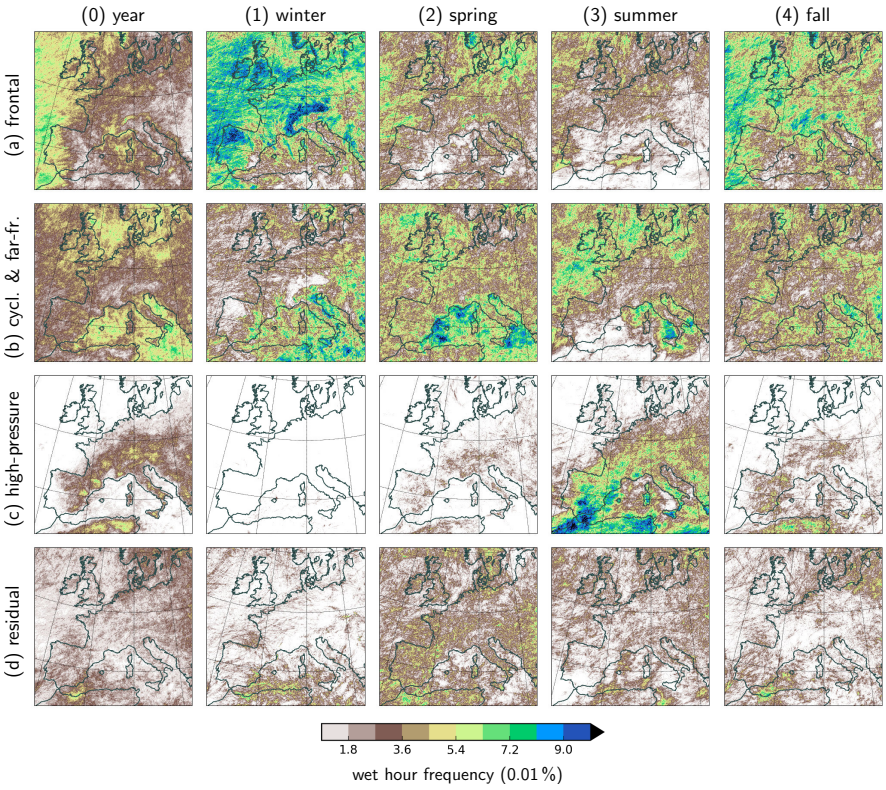

Figure S6. Like Fig. S5 b–d but for heavy precipitation, showing the frequency of hours with precipitation exceeding the local 99.9^{th} all-hour percentile of hourly precipitation.

~~Relative contributions to heavy precipitation, defined as the amount exceeding the local 99.9^{th} all-hour percentile of hourly precipitation intensity in a given season, during (1–4) each season of the nine-year period 2000–2008of front-cyclone-relative components: (a) sum of cold-frontal, warm-frontal, and collocated; (b) far-frontal; (c) cyclonic; (d) high-pressure; and (e) residual.~~